NASA Technical Memorandum 86843

Design of Adaptive Control Systems by Means of Self-Adjusting Transversal Filters

S.J. Merhav

February 1986

National Aeronautics and Space Administration

NASA Technical Memorandum 86843

Design of Adaptive Control Systems by Means of Self-Adjusting Transversal Filters

S. J. Merhav, Ames Research Center, Moffett Field, California

February 1986

National Aeronautics and
Space Administration

Ames Research Center
Moffett Field, California 94035

$d_j, d(\cdot)$	desired output of transversal filter
$e(\cdot)$	equation error in transversal filter
F_a, F_i	adaptation coefficients
$G(\cdot)$	transfer function of controller
$\hat{G}(\cdot)$	estimate of $G(\cdot)$
$i(\cdot)$	system input
i,j,k	index symbols
$M(\cdot)$	transfer function of open-loop model
N	number of weights in transversal filter
$n(\cdot)$	process noise
$P(\cdot)$	transfer function of plant
$\hat{P}(\cdot)$	estimate of $P(\cdot)$
$\hat{P}_c(\cdot)$	copy of $\hat{P}(\cdot)$
$p \triangleq d/dt$	differential operator
P	information vector
R	information matrix
s	Laplace operator
t	time
T_f	real-time length of transversal filter
$T_R(\cdot)$	transfer function of closed-loop model
tr	trace
$v(\cdot)$	measurement noise
$\underline{w}$	weight vector in the transversal filter

w_i	ith component in $\underline{w}$
$x(\cdot)$	input to transversal filter
$YF, y_j, y(\cdot)$	output of transversal filter
$z(\cdot)$	actual plant output
$z_m(\cdot)$	measured-plant output
ΔT	time increment
$\epsilon(\cdot)$	control system error
λ	eigenvalue
ω	natural frequency
μ	adaptation gain factor
$\underline{\nabla}$	gradient vector
σ_i	rms value of input
σ_n	rms value of noise
τ_{it}	convergence time constant in terms of iterations
τ	actual convergence time
ζ	damping coefficient

SUMMARY

This paper addresses the design of closed-loop adaptive control systems based on nonparametric identification. Implementation is by self-adjusting Least Mean Square (LMS) transversal filters. The design concept is Model Reference Adaptive Control (MRAC). Major issues are to preserve the linearity of the error equation of each LMS filter, and to prevent estimation bias that is due to process or measurement noise, thus providing necessary conditions for the convergence and stability of the control system. The controlled element is assumed to be asymptotically stable and minimum phase. Because of the nonparametric Finite Impulse Response (FIR) estimates provided by the LMS filters, a priori information on the plant model is needed only in broad terms.

The "Indirect Method," involving explicit plant identification, and the "Direct Method," in which the controller is directly computed, are compared in the light of filter and system constraints. Following a survey of control system configurations and filter design considerations, system implementation is shown here in Single Input Single Output (SISO) format which is readily extendable to multivariable forms. In extensive computer simulation studies the controlled element is represented by a second-order system with widely varying damping, natural frequency, and relative degree. Excellent convergence and robustness are demonstrated by the step response of the adapted system which deviates from the reference model by only a few percent under wide parameter variations of the controlled element. Controller FIR estimates and convergence time-histories support the validity of the concept.

INTRODUCTION

The principal approaches to the design of adaptive control systems require a priori knowledge of the order and relative degree of the controlled system. More specifically, to ensure convergence and stability, the transfer function of the error equation in the adaptive algorithm must be positive-real (refs. 1 and 2). Underlying the realization of an adaptive controller is parametric system identification. This may take the form of the "Indirect Method" (ref. 3), in which the unknown parameters of the plant are explicitly identified. Their estimates are used in the computation and adjustment of the controller parameters so as to meet the requirements of a suitable performance criterion. Alternatively, in the "Direct Method," the controller-plant system output is compared to that of a reference model. Their difference drives the adaptive algorithm which adjusts the controller. In either method, the plant is modeled by a finite-dimensional differential

equation. A substantial advantage of finite- dimensional modeling is the relatively fast convergence of the adaptive algorithm. A major disadvantage is that the controller design is complex and its performance strongly depends on the validity of the assumed form of the plant model (ref. 1). A major issue in the design of parametric adaptive controllers is the need to prevent parameter estimation bias caused by process or measurement noise.

An alternative approach to the design of adaptive control systems investigated in this paper is by nonparametric identification in the time domain. The controlled element is assumed to be linear, asymptotically stable, and minimum phase. Nonparametric, time-domain identification can be implemented by self-adjusting transversal filters (ref. 4). These filters consist of the weighted sums of linearly independent time functions derived from the system input. Of particular importance is the tapped delay line (ref. 4), which is a natural form in digital realizations. The weight vector constitutes a discrete approximation of the identified system in the form of a discrete Finite Impulse Response (FIR). Filters of this type, known as Least Mean Squares (LMS) filters, have been widely studied in the past two decades and have found extensive potential applications, in particular, in adaptive noise cancellation and in signal processing (ref. 5). More recently, lattice filters, which have superior convergence properties (ref. 6), are receiving increasing attention in signal processing and in noise cancellation.

Recently, the application of self-adjusting filters in control systems has been extensively studied in noise canceling (ref. 7), in parasitic mode suppression (ref. 8), and in adaptive control (refs. 9 and 10). The main advantage of this approach is that no precise assumptions on the form and order of the controlled plant are necessary. Distributed systems and lumped parameter systems are equally treated. The adaptive controller is implemented by a single algorithm which is applicable to dynamical systems with widely varying parameters and forms. A major issue is that to ensure convergence and provide stability, the implementation of the adaptation process, referred to herein as system configuration, must ensure the necessary conditions of linearity between the error and the weight vector in each individual filter and must permit realizable implementations of the adaptation process.

Another issue in the choice of the system configuration is the presence of process or measurement noise which may cause biased parameter estimates (ref. 10). Consequently, nonparametric adaptive-control system concepts in this class have resulted in essentially open-loop configurations (refs. 9 and 10). These configurations have the advantage of adaptively converging to a specified dynamic response which is dictated by a reference model while avoiding the constraints of design to stability as encountered in feedback structures. However, the crucial problem of process-noise suppression apparently has not been resolved in these open-loop design concepts.

It is the purpose of this study to apply the concept of nonparametric time-domain identification in the design of closed-loop adaptive control systems. It addresses design and implementation issues as outlined in the following sections. The first section is a brief outline of the problem statement. In the second

section, a number of system configurations are surveyed and candidate designs are pointed out in view of system and filter constraints. In the third section, LMS filter design is discussed in view of convergence time and closed-loop design criteria in relation to the number of weights and tap spacings. In the fourth section, system implementation is discussed for single-input-single-output (SISO) adaptive systems. It is indicated that in applications with substantial additive noise the indirect method, i.e., explicit plant identification is preferable. In applications with insignificant noise, the direct method is superior. In the fifth section, the performance of indirect and direct adaptive controllers is studied by means of computer simulations. A second-order plant serves as benchmark example. The results indicate excellent convergence to the reference model under wide variations of plant parameters and relative degree. Appendix A summarizes the principal properties of LMS filters. Appendix B addresses the effects of process and measurement noise in identification and adaptation.

The principal finding of this study is that nonparametric closed-loop adaptive control is feasible. In particular, the response of the adapted system demonstrates only minute deviations from the response of the specified reference model even when the damping coefficient of the second-order plant is varied from 10^{-3} to 1 and the relative degree is varied from one to two. Regarding the second-order example as a model of any of a number of modes in dynamical systems, the results indicate, among others, the potential of the method in adaptively suppressing parasitic oscillations caused by unmodeled modes, and to achieve highly robust control which is shaped to a specified desired form of response. The relatively low rate of convergence of the LMS filter applied in this study is of minor significance in space structures or in robotics applications. The issue of persistent excitation does not conflict with the normal operation in such applications. This excitation, which is applied only during conditioning or training periods, is removed during normal operation.

The results obtained encourage the extension of this study to multivariable and nonminimum phase systems and to the implementation of lattice filters for potentially faster convergence of the controller.

STATEMENT OF THE PROBLEM

The realization of a nonparametric adaptive control system based on LMS-type self-adjusting filters hinges on the fulfillment of a number of assumptions and conditions. These are first briefly stated here and are later discussed in further detail.

Assumptions

The following assumptions are made: (1) The plant is a linear, continuous-time, asymptotically stable, minimum-phase, lumped-parameter, or distributed-time varying system (2) persistent excitation is provided either by the system input or

by artificial wide-band identification signals; and (3) plant parameters may vary slowly in comparison with typical adaptation time constants, or they are piecewise constant.

Linearity of the Error Equation

As indicated in appendix A, the gradient algorithm underlying the operation of the LMS self-adjusting filter is determined by the error equation, as given in appendix A, in discrete form, where d_j is the desired output and where y_j is the actual filter output. $\underline{w}_j$ is the weight vector.

$$e_j = d_j - y_j = d_j - \underline{x}_j^T \underline{w}_j \tag{1}$$

Since the error equation is linear in $\underline{w}_j$, one has

$$\frac{\partial}{\partial \underline{w}} e_j \Big|_{\underline{w}=\underline{w}_j} = \underline{x}_j \tag{2}$$

which is independent of $\underline{w}_j$.

It is readily verified that this is a necessary condition for the convergence and stability of each self-adjusting filter in the system. Therefore, the incorporation of self-adjusting filters in the control system should not violate the linear relationship in equation (1). This can easily occur in closed-loop feedback configurations.

Filter Truncation Error

The controlled plant is assumed to be continuous-time, minimum phase and asymptotically stable. Its impulse response is therefore Infinite Impulse Response (IIR). In accordance with equation (A17) the error e_j, given by

$$e_j = d_j - \sum_{k=1}^{N} w_{kj} x(j - k + 1) \tag{3}$$

incorporates a residual truncation error. Consequently the gradient $\hat{\nabla}_j$ in equation (A4) and the weight increment in equation (A6) cannot vanish. Thus, under all operating conditions the filter must have the necessary real-time length to ensure that the truncation error will not cause excessive noise in the weight vector $\underline{w}_j$.

On the other hand, if the plant has lightly damped oscillatory modes, the number of weights N, must be sufficiently in excess of the lower limit set by the sampling theorem. Good fidelity of tracking d_j thus provided prevents an excessive error component in e_j which can increase parameter noise resulting in degraded performance.

Unbiasedness of the Plant Identification

A major issue in the realization of an adaptive control system often is unbiased identification of the plant in the presence of process or measurement noise. Noise components in closed-loop systems can give rise to circulating residuals which result in biased plant estimates. The controller that is determined from a biased plant model may perform poorly and may even cause instability.

Global Convergence and Stability of the Controller

The nonparametric modeling of the plant does not lend itself to formal expressions defining conditions for convergence and stability of the control system as is the case in parametric modeling. Therefore, if the necessary convergence conditions of each filter in the system are fulfilled, global convergence and stability of the complete control systems must still be assured by appropriate controller logic and by using the familiar convergence properties of LMS self-adjusting filters.

In view of the foregoing, it is the purpose of this study to investigate the feasibility and properties of an adaptive controller concept which is based on LMS-type self-adjusting filters which essentially meet all the indicated requirements, namely: (1) provision of closed-loop feedback control without violating the proper form of individual filters, i.e., linearity of the error equation; (2) filter design that ensures a sufficiently small truncation error and, when appropriate, provides sufficient fidelity so as to reproduce high-frequency modes; (3) provision of an identification algorithm which yields a unique and an unbiased estimate of the plant dynamics; and (4) design of the adaptive controller algorithm so as to meet the requirements of global convergence and stability.

SURVEY OF CONTROL SYSTEM CONFIGURATIONS

In this section candidate control systems configurations are discussed in view of the requirements in the problem statement section. The general approach is Model Reference Adaptive Control (MRAC). Various candidate configurations are first examined for the linearity of the error equation in $\underline{w}$, for biasedness caused by process or by measurement noise and the realizability of the gradient $\hat{\underline{\nabla}}$ in accordance with equation (A4). Both open-loop and closed-loop configurations are discussed. The differential operator $p \triangleq d/dt$ is used in the continuous-time system formulation. Finally, the configurations which essentially meet the foregoing requirements are selected.

Open-Loop MRAC

An apparently straightforward open-loop MRAC configuration is shown in figure 1.

M(p) is a linear reference model, P(p) is the controlled plant, and G(p) is an adaptive controller structured as an LMS transversal filter formulated here, for brevity, in continuous-time. The plant output is z(t) and n(t) is output-referred additive noise. The adaptation process is to adjust G(p) so that $G(p)P(p) \rightarrow M(p)$. In accordance with appendix A, G(p) is formulated as the weighted sum

$$G(p) = \sum_{i=1}^{N} g_i(p) w_{gi} \tag{4}$$

where $g_i(p)$ is the required set of linear operators which generate a set of linearly independent functions from the input i(t). The error $e(t) = r(t) - z(t)$ is

$$e(t) = \left[M(p) - P(p) \sum_{i=1}^{N} g_i(p) w_{gi} \right] i(t) - n(t) \tag{5}$$

e(t) is measurable and it fulfills the necessary condition of linearity in $\underline{w} \triangleq [w_1, w_2, \ldots, w_N]^T$. Furthermore, in the realization of $\hat{\underline{\nabla}}$, in accordance with appendix A, n(t) is absent in the operator

$$\frac{\partial e}{\partial w_{gi}} = -P(p) g_i(p) i(t) \qquad (i = 1,N) \tag{6}$$

This implies unbiasedness since $e\partial e/\partial w_i$ would not involve $n^2(t)$ terms. However, equation (6) implies, that to generate the N right-hand side partial derivatives, every component $g_i(p)i(t)$ must individually be first filtered by the unknown P(p). Observing figure 1 this is evidently not realizable and the algorithm cannot be implemented.

An alternative configuration of open loop MRAC as described in reference 10 is shown in figure 2. The order of P(p) and the adjustable controller G(p) is reversed and an exact copy $G_c(p) = G(p)$ precedes P(p), thus acting as the controller. The error $e(t) = r(t) - y(t)$ is

$$e(t) = [M(P) - G(p)P(p)]G(p)i(t) - G(p)n(t) \tag{7}$$

which is nonlinear in G(p). Thus, in the implementation of the gradient $\hat{\underline{\nabla}}$, we now have

$$\frac{\partial e}{\partial w_{gi}} = \frac{\partial e}{\partial G(p)} \frac{\partial G(p)}{\partial w_{gi}} i(t) \tag{8}$$

In view of equation (4),

$$\frac{\partial G(p)}{\partial w_{gi}} = g_i(p) \tag{9}$$

and

$$\frac{\partial e}{\partial G(p)} = [M(p) - G(p)P(p)]i(t) - P(p)G(p)i(t) - n(t) \tag{10}$$

From equations (8)-(10), $\partial e/\partial w_{gi}$ can be written as

$$\frac{\partial e}{\partial w_{gi}} = [M(p) - G(p)P(p)]g_i(p)i(t) - P(p)G(p)g_i(p)i(t) - g_i(p)n(t) \tag{11}$$

The following observations apply to equation (11):

1. It is the second term which represents the desired signal, i.e., the actual output of the filter $g_i(p)$, $i = 1,N$, which is essential in the computation of the gradient $\hat{\underline{\nabla}}$. It is realizable since $P(p)$ actually precedes $G(p)$.

2. The first term is directly related to $e(t)$ and vanishes if $e(t) \to 0$.

3. The third term incorporates a noise term caused by $n(t)$.

4. The partial derivative $\partial e/\partial w_{gi}$ is a function of $G(p)$, and thus of $\underline{w}$.

5. The product $e\partial e/\partial w_{gi}$ incorporates terms with $n^2(t)$.

Consequently, the configuration shown in figure 2, though providing a realizable $\partial e/\partial w_{gi}$, would yield biased values for $G(p)$ and since $\partial e/\partial w_{gi}$ is a function of $\underline{w}_g$, convergence and stability of the algorithm is not assured.

The foregoing obstacles result from this attempt to estimate $G(p)$ directly from $P(p)$ and to simultaneously implement adaptive control in the presence of additive noise $n(t)$.

These obstacles can be avoided by introducing explicit plant identification as an intermediate step. As shown in figure 3, the model $\hat{P}(p)$ thus identified, is used to compute $G(p)$ which controls the plant $P(p)$ (ref. 11).

Figure 3(a) represents the plant identification. Figure 3(b) represents the controller computation: $i(t)$ is the plant input and $u(t)$ is an optional excitation signal, preferably white noise. The LMS filter assigned to plant identification is formulated by

$$\hat{P}(p) = \sum_{i=1}^{N} p_i(p)w_{pi} \tag{12}$$

The error $e_p(t)$ is

$$e_p(t) = z(t) - y(t) = [P(p) - \hat{P}(p)]i(t) + n(t)$$

$$= P(p)i(t) - \left[\sum_{i=1}^{N} p_i(p)w_{pi}\right]i(t) + n(t) \tag{13}$$

Thus, since

$$\frac{\partial e_p(t)}{\partial w_{pi}} = -p_i(p)i(t) \tag{14}$$

is free of additive noise and independent of $\underline{w}_p$, the identification algorithm fulfills the necessary conditions for global convergence, stability, and unbiasedness. Furthermore, equation (14) is realizable.

For figure 3(b) we have

$$e_G(t) = [M(p) - G(p)\hat{P}_c(p)]u(t) \tag{15}$$

where $\hat{P}_c(p)$ is a copy of $\hat{\underline{P}}(p)$. In view of equation (4),

$$\frac{\partial e_G(t)}{\partial w_{gi}} = -g_i(p)\hat{P}_c(p)u(t) \tag{16}$$

The plant identification given by $\hat{P}(p)$ contains noise components $\tilde{w}_p$ in the parameter vector $\underline{w}_p$ which are reflected in $\hat{P}_c(p)$. Thus, the estimate $\hat{P}_c(p)$ can be expressed as

$$\hat{P}_c(p) = P(p) + \tilde{P}_c(p) \tag{17}$$

where $\tilde{P}_c(p)$ is the random fluctuation of $\hat{P}_c(p)$ resulting from the parametric noise $\tilde{w}_p$ contributing noise components $\tilde{\underline{w}}_p u(t)$. These noise components are modulative, and do not cause estimation bias. Therefore, the right-hand side in equation (16) fulfills the necessary conditions for global convergence, stability, and unbiasedness. Thus, G(p) converges to the desired solution

$$G(p) \to \frac{M(p)}{\hat{P}_c(p)} \tag{18}$$

where G(p) is copied to $G_c(p)$ which acts as the actual controller at the plant input, as shown in figure 3(a).

Finally, the plant output z(t) is given by:

$$z(t) = G_c(p)P(p)i(t) + n(t)$$

$$= M(p)\frac{P(p)}{\hat{P}_c(p)}\, i(t) + n(t) \simeq M(p)i(t) + n(t) \qquad (19)$$

The configuration shown in figure 3, therefore, provides a stable unbiased adaptive controller which implements the dynamic response of a desired model M(p). This kind of open-loop control could, in principle, be applied when process or measurement noise is negligibly small. Of the three classical objectives of control systems, i.e., response shaping, reduction of sensitivity to plant parameter variations and noise suppression, it meets only the first two. Moreover, from equation (19) it is evident that the parametric noise in $P_c(p)$ is directly reflected in z(t). Consequently, this open-loop configuration cannot be considered as a complete solution to the adaptive control problem.

Closed-Loop Configurations

From the previous paragraph, explicit plant identification appears to be essential in the implementation of adaptive control. Process noise suppression must be provided by negative feedback. An obvious closed-loop configuration would be of the form shown in figure 4, which can be considered as an extension of figure 3. Since closed-loop systems are considered, process noise n(t) and measurement noise v(t) are introduced separately. It is easily verified that

$$z(t) = \frac{G(p)P(p)}{1 + G(p)P(p)}\,[i(t) - v(t)] + \frac{1}{1 + G(p)P(p)}\, n(t) \qquad (20)$$

$$z_m(t) = \frac{G(p)P(p)}{1 + G(p)P(p)}\, i(t) + \frac{1}{1 + G(p)P(p)}\,[n(t) + v(t)] \qquad (21)$$

where

i(t) system input

z(t) physical plant output

$z_m(t)$ measured plant output

n(t) process noise referred to the output

v(t) measurement noise

Thus, with respect to the actual output $z(t)$, $v(t)$ is equivalent to the input $i(t)$. However, with respect to the measured output $z_m(t)$, $v(t)$ is equivalent to the process noise $n(t)$.

It is readily verified that

$$e(t) = \frac{G(p)}{1 + G(p)P(p)} [P(p) - \hat{P}(p)]i(t) + \frac{1 + G(p)\hat{P}(p)}{1 + G(p)P(p)} [n(t) + v(t)] \qquad (22)$$

In equation (22), it is only the input signal $i(t)$ which is common to $P(p)$, and to $\hat{P}(p)$, thus providing the required persistent excitation for plant identification. Neither $n(t)$ nor $v(t)$ are valid identification signals. Equation (22), which is the error equation of the closed-loop systems, is linear in $\hat{P}(p)$. However, the partial derivative

$$\frac{\partial e(t)}{\partial \hat{P}(p)} = \frac{G(p)}{1 + G(p)P(p)} i(t) + \frac{G(p)}{1 + G(p)P(p)} [n(t) + v(t)] \qquad (23)$$

contains the additive noise $n(t) + v(t)$ so that the gradient $\hat{\underline{v}} = e\partial e/\partial \hat{P}(p)$ contains terms with $[n(t) + v(t)]^2$ causing a bias in $\hat{P}(p)$. Thus, direct plant identification in a noisy closed loop results in a biased plant estimate and yields a biased controller.

Moreover, observation of equation (22) discloses that the signal $\varepsilon(t) = [G(p)/[1 + G(p)P(p)]i(t)$ in general does not provide an efficient identification signal. Since $G(p)P(p) >> 1$ is required in the useful frequency region, it follows that $\varepsilon(t)$ does not efficiently excite the modes of $P(p)$. Consequently, a relatively slow convergence of the weights $\underline{w}_p$ in $\hat{P}(p)$ cannot be avoided. Thus, the straightforward approach of closed-loop identification as embodied in figure 4 is bound to yield slow and biased plant parameter estimation. In the sequel it is shown how this problem is overcome in conjunction with the adaptive control process.

An alternative approach would be to identify the closed-loop system $T(p)$ and to compute the plant $P(p)$ from this identified model. The concept of this configuration is shown in figure 5.

The closed-loop transfer function is

$$T(p) = \frac{G(p)P(p)}{1 + G(p)P(p)} \qquad (24)$$

the error equation, in view of equations (21) and (24) is

$$e(t) = [T(p) - \hat{T}(p)]i(t) + \frac{T(p)}{G(p)P(p)}[n(t) + v(t)] \tag{25}$$

Denoting

$$\hat{T}(p) = \sum_{i=1}^{N} t_i(p)w_{Ti}$$

we have

$$\frac{\partial e(t)}{\partial w_{Ti}} = -t_i(p) \tag{26}$$

Since $\partial e/\partial \underline{w}_{Ti}$ is noise-free and independent of $\underline{w}^T$, the necessary conditions for unbiased convergence of $\hat{T}(p) \rightarrow T(p)$ are fulfilled.

From a copy $\hat{T}_c(p)$ of $\hat{T}(p)$ it is possible to obtain the estimate $[G(p)P(p)]\hat{}$ by the inverse operation

$$[G(p)P(p)]\hat{} = \frac{\hat{T}_c(p)}{1 - \hat{T}_c(p)} \tag{27}$$

Besides being extremely sensitive to uncertainties in $\hat{T}(p)$, the estimated term $[G(p)P(p)]\hat{}$ obviously does not provide a realizable solution for $G(p)$.

The Indirect Method

It remains to obtain an unbiased estimate $\hat{P}(p)$ from $\hat{T}(p)$. A method to accomplish this is described in figure 6.

In the closed-loop control system (fig. 6(a)) excited by $i(t)$, $\hat{T}_1(p)$ and $\hat{T}_2(p)$ provide the estimates of

$$T_1(p) = \frac{P(p)}{1 + G_c(p)P(p)} \tag{28}$$

$$T_2(p) = \frac{1}{1 + G_c(p)P(p)} \tag{29}$$

The signal $r(t) = G_c(p)i(t)$ is noise-free, and the errors $e_1(t)$ and $e_2(t)$ are given by

$$e_1(t) = \left[T_1(p) - \sum_{i=1}^{N} t_{1i}(p) w_{T_{1i}}\right] r(t) \tag{30}$$

$$e_2(t) = \left[T_2(p) - \sum_{i=1}^{N} t_{2i}(p) w_{T_{2i}}\right] r(t) \tag{31}$$

The noise terms that are due to $n(t)$ and $v(t)$ in equations (30) and (31) are disregarded here since they do not cause biased estimates. It follows that

$$\frac{\partial e_1(t)}{\partial w_{T_{1i}}} = -t_{1i}(p) r(t) \tag{32}$$

$$\frac{\partial e_2(t)}{\partial w_{T_{2i}}} = -t_{2i}(p) r(t) \tag{33}$$

are noise-free and independent of $\underline{w}_{T1}$ and $\underline{w}_{T2}$, respectively. Therefore, estimates $\hat{T}_1(p)$ and $\hat{T}_2(p)$ are unbiased and globally convergent and stable. The estimates $\hat{T}_1(p)$ and $\hat{T}_2(p)$ are copied to $\hat{T}_{1c}(p)$ and $\hat{T}_{2c}(p)$, respectively, as shown in figure 6(b). The estimate $\hat{P}(p)$ is obtained as follows: $\hat{T}_{1c}(p)$ serves as the reference model. The error

$$e_3(t) = [\hat{P}(p)\hat{T}_{2c}(p) - \hat{T}_{1c}(p)]u(t) \tag{34}$$

converges in the mean to zero so that

$$\hat{P}(p)\hat{T}_{2c}(p) \to \hat{T}_{1c}(p) \tag{35}$$

implying that

$$\hat{P}(p) = \frac{\hat{T}_{1c}(p)}{\hat{T}_{2c}(p)} \tag{36}$$

Since $\hat{T}_{1c}(p) \to T_1(p)$ and $\hat{T}_{2c}(p) \to T_2(p)$, it follows from equations (36), (28), and (29) that

$$\hat{P}(p) \to \frac{P(p)/[1 + G_c(p)P(p)]}{1/[1 + G_c(p)P(p)]} = P(p) \tag{37}$$

This two-stage identification process is interesting in that variations in $G_c(p)$, in particular if they are slow, are only weakly reflected in the estimate $\hat{P}(p)$.

For $G_c(p)$ = constant, the algorithm that is determined by equation (34) will, in general, converge relatively slowly. The reason for this is that the signal $s(t)$ exciting $\hat{P}(p)$ in figure 6(b) is given by

$$s(t) = \hat{T}_{2c}(p)u(t) \approx \frac{1}{1 + G_c(p)P(p)}\, u(t) \tag{38}$$

In particular, if $G_c(p)P(p) >> 1$, the spectrum of $s(t)$ has zeros in the vicinity of the poles of $P(p)$. Therefore, $s(t)$ has only minute power in the required frequency range and therefore does not provide sufficient excitation. The resulting slow convergence is a disadvantage in real-time applications as needed in adaptive control. This deficiency is equivalent to the one discussed in conjunction with $\varepsilon(t)$ in figure 4.

The problem is inherently overcome by the implementation of loop (c) in figure 6. Let $M(p)$ be the reference model of the open-loop transfer function designed for the desired closed-loop response $T_R(p)$. $G(p)$ is structured as a transversal filter

$$G(p) = \sum_{i=1}^{N} g_i(p)w_{gi}$$

The error $e_4(t)$ is

$$e_4(t) = [M(p) - \hat{P}_c G(p)]u(t) \tag{39}$$

and

$$\frac{\partial e_4(t)}{\partial w_{gi}} = -g_i(p)\hat{P}_c(p)u(t) \tag{40}$$

which is noise-free and independent of $\underline{w}_g$. Thus global convergence for (c) is assured and

$$\hat{P}_c(p)G(p) \to M(p) \tag{41}$$

$G_c(p)$ is a copy of $G(p)$. Therefore, in the actual control system (a) one has

$$P(p)G_c(p) \approx M(p) \tag{42}$$

It follows that (c) provides the required controller adaptation algorithm. Moreover, with the implementation of (c), $s(t)$ in equation (6), defined in equation (38) is modified to

$$s(t) \simeq \frac{1}{1 + M(p)}\, u(t) \tag{43}$$

In equation (43) the plant zeros previously mentioned are canceled. Thus, the convergence of $\hat{P}_c(p)G(p)$ to $M(p)$ in equation (41) accelerates the convergence of $\hat{P}(p)$ which, in turn, further accelerates the convergence of $G(p)$. This self-reinforcing process is in effect under the assumption that $P(p)G_c(p)$ is sufficiently close to $M(p)$ to assure the stability of the control system. To justify this assumption two requirements have to be fulfilled: (1) variations in $P(p)$ are sufficiently slow with respect to the adaptation time constants of loops (b) and (c) in figure 6, and (2) an appropriate initialization procedure is required in order to ensure proper convergence on start-up of the system.

The foregoing leads to the conclusion that efficient closed-loop plant identification for real-time performance is, in principle, inseparable from the adaptation problem. Subject to the assumptions made, the implementation shown in figure 6 is a valid configuration. In the sequel it will be referred to as configuration 1.

FILTER DESIGN CONSIDERATIONS

As shown in the section on Survey of Control-System Configurations, for the indirect method the crucial element in the implementation of adaptive control is the accurate identification of the plant. This section addresses the essential design considerations in the realization of adaptive filters that are suitable for real-time plant identification as required in adaptive control. The principal factors involved are time of convergence, number of weights, misadjustment, FIR truncation error, and effective bandwidth.

Normalization

Observing equation (A3) in appendix A, it is obvious that the eigenvalues of R, $\lambda_1, \lambda_2, \ldots, \lambda_N$ are given by $E[\underline{x}_j \underline{x}_j^T]$, i.e., they are quadratic functions of the input $x(t)$. Thus, speed of convergence is fundamentally very sensitive to the input power level. More specifically, the average exponential convergence time-constant τ_{it} in terms of the number of iterations defined in equation (A15) is

$$\tau_{it} = \frac{N}{4\mu \mathrm{tr} R} \tag{44}$$

equation (44) underlines that the representative time-constant for a given fixed gain is inversely proportional to the total incident input power given by R (ref. 5).

Since, in control systems, R may vary widely, it is desirable to make τ_{it} independent of R. This can be achieved by normalization. Observing the permitted upper bound on μ in equation (A14), we determine it by

$$\mu = \frac{1}{FtrR} \tag{45}$$

where $F \geq 1$ is a constant coefficient. Substituting equation (45) into equation (44), we have

$$\tau_{it} = \frac{NF}{4} \tag{46}$$

Thus, τ_{it} is determined by the design parameter F. Equation (45) is easily implemented in the on-line algorithm from the components $x_{1j}, x_{2j}, \ldots, x_{Nj}$, trR can be computed on line by

$$trR_j = \sum_{i=1}^{N} x_{ij}^2 \tag{47}$$

This independence of τ_{it} on input power plays an essential role in the realization of the adaptive control algorithm discussed later.

Misadjustment and Additive Noise

The requirement $F \geq 1$ dictates the theoretical lower bound with regard to the stability of the LMS algorithm. The actual lower bound, however, is determined by the parameter noise that is due to the misadjustment M as defined in equation (A18), appendix A. Thus, for a given acceptable misadjustment M, F is determined by

$$F \geq \frac{1}{M} \tag{48}$$

For example, if the permitted misadjustment is $M = 0.05$, then $F \geq 20$. The upper bound of F is dictated by the convergence time-constant τ_{it} given in equation (46). In this work we define $\tau_c = 4\tau_{it}$ to assure convergence within ~2% of the asymptotic value of the estimate. Thus, $\tau_c = NF$. For a given acceptable value of τ_c, we therefore have $F \leq \tau_c/N$. Consequently, the choice of F is bounded by

$$\tau_c/N \geq F \geq 1/M \tag{49}$$

Clearly, equation (49) implies that the lower bound of τ_c is

$$\tau_c \geq N/M \tag{50}$$

Thus, for example, if $N = 50$, $M = 0.05$, $\tau_c \geq 1000$ (iterations). In addition to M, the effect of additive process or measurement noise must be considered. With $n(t)$ and $v(t)$ present, the error is

$$e_j = d_j - \underline{x}_j^T \underline{w}_j + n_j + v_j \tag{51}$$

Accordingly, the gradient would include the noise component

$$\hat{\underline{\nabla}}_{nj} = -2(n_j + v_j)\underline{x}_j \tag{52}$$

The corresponding parameter noise component is

$$\tilde{\underline{w}}_j = 2\mu(n_j + v_j)\underline{x}_j = \frac{2}{FtrR}(n_j + v_j)\underline{x}_j \tag{53}$$

Equation (49) indicates that the actual lower bound of F may be greater than $1/M$, eventually causing a corresponding increase in τ_c. Thus, the actual increase of F above $1/M$ must be determined by a priori estimates of expected noise levels in the system. The principal effect of normalizing the LMS algorithm by equation (A9) is that for a given F, both τ_c and $\tilde{\underline{w}}_j$ are made invariant to input power variations. This property is crucial in assuring convergence of the control system.

Principal Filter Parameters

The principal design parameters are

N the number of weights w_i, $i = 1,N$

T_f the total real time length of the filter delay line

ΔT the tap spacing between x_i, x_{i+1} . . .

Some ground rules, especially applicable to filtering and signal processing are given in reference 5. They relate T_f and ΔT to signal band width and frequency resolution.

In the control oriented identification problem discussed here, somewhat different ground rules are needed. The impulse response for asymptotically stable plants is broadly characterized by exponentially decaying time-functions. Therefore, the FIR nature of the finite length delay line involves a truncation error, which, if excessive, prevents proper convergence of the parameter vector $\underline{w}$. To ensure a sufficiently small truncation error, the following design rule will be adopted:

Let $\mathrm{Re}(\lambda\min)$ be the real part of the smallest expected eigenvalue of $P(p)$. Choosing $T_f \geq 4[\mathrm{Re}(\lambda\min)]^{-1}$ ensures that the truncation error is less than 2%. The next design consideration is the tap spacing ΔT. Its upper bound is dictated by the input signal bandwidth ω_i as determined by the sampling theorem, i.e.,

$$\Delta T \leq \frac{1}{2f_i} = \frac{\pi}{\omega_i} \tag{54}$$

Thus, the smallest number of taps N is given by

$$N = T_f/\Delta T + 1 \tag{55}$$

Since normally $N \gg 1$, in the sequel N is approximated by $N = T_f/\Delta T$. Control systems design considerations generally impose further requirements for ΔT. Let ω_p be the cut-off frequency of the plant $P(p)$. In accordance with control systems design practice for stability and robustness, the model $\hat{P}(p)$ must reproduce the output frequency components of $P(p)$ out to approximately $10\omega_p$. This implies that the tap spacing must meet the condition

$$\Delta T \leq \frac{1}{2f_p} = \frac{\pi}{10\omega_p} \tag{56}$$

For example, assuming a simple first-order plant $P(s) = \omega_p/(s + \omega_p)$, $\mathrm{Re}(\lambda\min) = \omega_p$ implying $T_f \geq 4/\omega_p$. Thus

$$N = \frac{T_f}{\Delta T} = \frac{4}{\omega_p} \Big/ \left(\frac{\pi}{10\omega_p}\right) = \frac{40}{\pi} \simeq 13 \tag{57}$$

The significance of equation (56) is that ΔT determines the tap density at the leading edge of the FIR which represents the required high-frequency response of the plant.

As a second example, applying the same design rule to a lightly damped second-order system

$$P(s) = \omega_p^2/(s^2 + 2\omega_p\zeta_p s + \omega_p^2)$$

yields $\mathrm{Re}(\lambda\min) = \omega_p\zeta_p$. Thus, for example, $\zeta_p = 0.1$,

$$N = \frac{T_f}{\Delta T} = \frac{4}{\omega_p\zeta_p} \Big/ \left(\frac{\pi}{10\omega_p}\right) = \frac{40}{\zeta_p\pi} \simeq 130 \tag{58}$$

To ensure good fidelity of the FIR provided by the filter, we examine the number of weights per cycle n in the IIR. The period is $T_p = 2\pi/\omega_p$ and the number of cycles n_c within T_f is

$$n_c = \frac{T_f}{T_p} = \frac{4}{\omega_p \zeta_p} \frac{\omega_p}{2\pi} = \frac{2}{\pi \zeta_p} \tag{59}$$

In accordance with equation (58), $n = N/n_c = (40/\zeta_p \pi)(\pi \zeta_p/2) = 20$, which is adequate.

It should be noted that for the mere estimation of ω_p and ζ_p, the sampling theorem would not require more than $n = 2$. However, the fidelity of the FIR would be poor with the result of sustaining a substantial error ε_j and, possibly, excessive parameter noise $\tilde{\underline{w}}_j$ (see appendix A). The foregoing is illustrated in figure 7 for $T_f = 6$ sec and $P(s) = 25/(s^2 + 1s + 25)$, i.e., $\omega_p = 5$. $\zeta_p = 0.1$, $T_p = 2\pi/\omega_p = 1.256$ sec; thus $n_c = 6/1.256 = 4.77$. Figure 7(a) illustrates the computed IIR. Figure 7(c) shows the estimated FIR for an arbitrary $N = 40$ resulting in $n = 40/4.77 = 8.38$ indicating poor fidelity. Figure 7(b) shows the estimated FIR for an arbitrary $N = 120$ for which $n = 25.14$, indicating good fidelity and complying with the design value $n = 20$.

In general the plant may have a number of modes. Denoting

$$\Lambda = \frac{\mathrm{Re}(\lambda \mathrm{max})}{\mathrm{Re}(\lambda \mathrm{min})} \tag{60}$$

In accordance with equation (57), the required number of weights N would be

$$N = \frac{40}{\pi} \Lambda \tag{61}$$

It follows that the need for N in excess of 100 can be easily encountered. If the expected IIR of $P(s)$ is of aperiodic nature, the problem of an excessive N can be remedied by nonuniform spacing. The highest tap density is assigned to the neighborhood of the leading edge, gradually spreading out toward the trailing edge. A simple form of implementation can be, for example, by subdividing T_f into four sections and using a tap sequence such as 1, 2, 3, 4. This would yield the relation

$$T_f = \frac{1}{4}(1 + 2 + 3 + 4) = 2.5N \, \Delta T$$

or

$$N = \frac{1}{2.5} \frac{T_f}{\Delta T} \tag{62}$$

Thus, a considerable saving in weights can be obtained without compromising filter fidelity.

The actual time of convergence τ (sec) is determined by equation (49), i.e., τ_c and ΔT. Thus, $\tau = \tau_c \Delta T$. Substituting the appropriate values for τ_c and ΔT, we have for a uniformly spaced filter

$$\tau = NF \frac{T_f}{N} = FT_f \tag{63}$$

or for a nonuniformly spaced filter as given in equation (62).

$$\tau = 0.4FT_f \tag{64}$$

Thus, the real convergence time is determined by the product of the filter length T_f and the coefficient F irrespective of the number of weights N.

SYSTEM IMPLEMENTATION

In this section the integration of the reference model $T_R(p)$ and the LMS-filter-based adaptive controller is described. The issue of bounds on the level of control activity is not addressed here. These are regarded as part of the design of the reference model. Here, $T_R(p)$ having a satisfactory dynamic response is chosen for the purpose of illustration. An example of a second-order plant $P(p)$ is chosen to provide explicit solutions for the controller. These choices of $P(p)$ and $T_R(p)$ also serve in the simulation examples presented in the section on Computer Simulation Tests. Three system configurations are discussed and are described in figures 8-10, in which, for the sake of simplicity, noise is represented by $n(t)$ alone.

The open-loop reference model $M(p)$ is determined from the specified closed-loop system $T_R(p)$ relating the input $i(t)$ to the output $z(t)$. The relationship between $M(p)$ and $T_R(p)$ in transfer function format being

$$T_R(s) = \frac{M(s)}{1 + M(s)} \tag{65}$$

Two requirements must be met:

$$\lim_{s \to 0} T_R(s) = 1 \tag{66}$$

$$\lim_{s \to 0} M(s) = \text{constant} \tag{67}$$

The first is the standard specification in closed loop control. The second assures the boundedness of loop (c) in figure 6. In view of equation (65), equations (66) and (67) are not compatible unless integral control is introduced in series with the plant P(p). Thus, equation (65) is modified to

$$T_R(s) = \frac{M(s)/s}{1 + M(s)/s} = \frac{M(s)}{s + M(s)} \tag{68}$$

The solution for M(s) is

$$M(s) = \frac{sT_r(s)}{1 - T_R(s)} \tag{69}$$

We introduce the following example

$$T_R(s) \frac{10}{s^3 + 6.5s^2 + 9s + 10} \tag{70}$$

so that

$$M(s) = \frac{10}{s^2 + 6.5s + 9} \tag{71}$$

Assume that the plant is

$$P(s) = \frac{25}{s^2 + 2s + 25} \tag{72}$$

Then, in accordance with equation (42), the controller should converge to

$$G(s) = \frac{M(s)}{P(s)} = 0.4 \frac{s^2 + 2s + 25}{s^2 + 6.5s + 9} \tag{73}$$

In view of the conclusions on identifiability of closed-loop systems in the section on Survey of Control-System Configuration, and the basic Indirect Method shown in figure 6, the design of the adaptive control system is shown in figure 8. The control system (a) starts with the "switches" in position 1 which is the system initialization state. The system incorporates an integrator in series with P(p).

G_o is an arbitrary constant coefficient. The transfer functions $z(s)/G_o i(s)$ and $\epsilon_i(s)/G_o i(s)$ are

$$\frac{1}{G_o}\frac{z(s)}{i(s)} = T_1(s) = \frac{P(s)}{s + M(s)} \tag{74}$$

$$\frac{1}{G_o}\frac{\varepsilon i(s)}{i(s)} = T_2(s) = \frac{1}{s + M(s)} \tag{75}$$

$\hat{T}_1(s)$ and $\hat{T}_2(s)$ are their respective estimates provided by LMS filters, adjusted by $e_1(t)$ and $e_2(t)$, respectively. In state 1, the system operates in an open-loop mode. The input $i(t)$ is shaped by $M(s)$, and conditions $\hat{T}_1(s)$ and $\hat{T}_2(s)$ to their desired forms given in equations (74) and (75) which exist in the subsequent converged closed loop of state 2. This design concept will be referred to in the sequel as configuration 1. The spectrum of $s(t)$ indicated in figure 8(b), in view of equation (43) does not have notches in the neighborhood of the modes of $P(p)$, and therefore it can provide persistent excitation for the identification $\hat{P}(p)$. The convergence in the mean to zero of $e_3(t)$ in equation (34) yields the relation

$$\hat{P}(s) \to \frac{\hat{T}_{1c}(s)}{\hat{T}_{2c}(s)} = \frac{\{P(s)/[s + M(s)]\}\hat{}}{\{1/[s + M(s)]\}\hat{}} \approx P(s) \tag{76}$$

The last expression indicates that imperfections in $\hat{T}_{1c}(s)$ and $\hat{T}_{2c}(s)$ such as incomplete convergence tend to cancel so that $\hat{P}(s)$ converges to $P(s)$ more rapidly than does $\hat{T}_1(s)$ to $T_1(s)$ or $\hat{T}_2(s)$ to $T_2(s)$. This effect is demonstrated in simulated results not included in this paper.

With $\hat{P}(s) \to P(s)$, the copy $\hat{P}_c(s)$ in (C) conditions $G(s)$ so that

$$G(s)\hat{P}_c(s) \to M(s) \tag{77}$$

By using a suitable measure of the error $e_4(t)$ normalized to $u(t)$, convergence of equation (77) can be established and the control system switches to the closed-loop operational state 2. The abrupt jump from G_o to $G_c(p)$ causes a sudden change in the statistics of the input signal. However, if $\hat{T}_1(p)$ and $\hat{T}_2(p)$ have sufficiently converged, only minor transients are induced in $e_1(t)$ and $e_2(t)$, and consequently the estimate $\hat{P}(s)$ shows only a minor transient perturbation.

Henceforth, in state 2, the estimation of $T_1(s)$ and $T_2(s)$ proceeds on the basis of the open-loop transfer function $G_c(s)P(s)$ which is approximately equal to $M(s)$. Thus continuing estimates of $P(s)$ are obtained by

$$\hat{P}(s) = \frac{\hat{T}_{1c}(s)}{\hat{T}_{2c}(s)} = \frac{\{P(s)/[1 + G_c(s)P(s)]\}\hat{}}{\{1/[1 + G_c(s)P(s)]\}\hat{}} \tag{78}$$

The example of G(s) in equation (73) serves to underline a significant point with regard to the potential precision obtainable from the G(s) filter. In the foregoing it is tacitly assumed that all the filter lengths T_f in figure 8 are equal. In accordance with the section of Filter Design Control, T_f is initially determined by $[\mathrm{Re}\lambda\mathrm{min}]^{-1}$ of P(s), specifically $T_f \simeq 5[\mathrm{Re}(\lambda\mathrm{min})]^{-1}$. In the foregoing example in which $\omega_p \zeta_p = 1$, $T_f = 5/1 = 5$ sec. However, in equation (73), $\mathrm{Re}[\lambda\mathrm{min}] = 2$; thus, the convergence of the impulse response of G(s) is complete within $T_G = 5/2 = 2.5$ sec. If the filter consists, e.g., of N = 50 weights, the number of weights actually assigned to represent G(s) would be $50 \cdot T_G/T_f$. Considering the initial spike of the IR of a form such as in equation (72), the number of weights actually assigned to G(s) may not provide the required fidelity. This may become a severe limitation if the desired bandwidth of $T_R(s)$ and the resulting M(s) is too high.

An alternative approach to the Indirect Method described above is described in figure 9. In essence it is in the class of the Indirect Method MRAC based on the closed-loop reference model $T_R(s) = M(s)/[s + M(s)]$, although P(s) is not explicitly identified and the controller is directly determined by $T_R(s)$. With the control system (a) in position 1 the transfer function

$$T_1(s) = \frac{P(s)}{s + M(s)} \tag{79}$$

is estimated. M(s) is a priori determined from $M(s) = sT_R(s)/[1 - T_R(s)]$ as before. Simultaneously, (b) implements

$$\hat{T}_{1c}G(s) \rightarrow T_R(s) \tag{80}$$

or, explicitly

$$\left[\frac{P(s)}{s + M(s)}\right]\hat{}\,G(s) \rightarrow \frac{M(s)}{s + M(s)} \tag{81}$$

The last expression approximates the required relationship $\hat{P}(s)G(s) \rightarrow M(s)$ as provided by explicit plant identification shown in figure 6.

When G(s) is sufficiently close to M(s)/P(s), the system switches to state 2 and henceforth operates in the mode of a closed-loop MRAC. The implementation is considerably simpler than the explicit form of figure 8 since only two adaptation loops driven by $e_1(t)$ and $e_2(t)$ are required. This design concept will be referred to as configuration 2.

In applications where the additive noise n(t) is small a further simplification of the system is permitted. Its block diagram is shown in figure 10. The closed-loop reference model $T_R(s)$ is connected to the control system input at point I. The controller G(s) is directly identified from the signals at points II

and III. In the initialization phase 1, the system is driven via a fixed arbitrary gain G_o. The transfer function from point I to II is

$$T_1(s) = \frac{P(s)}{s + M(s)} \tag{82}$$

The reference model, with points I and III as its input and output, respectively, is

$$T_R(s) = \frac{M(s)}{s + M(s)} \tag{83}$$

The error e(t) drives the LMS algorithm of the controller G(s) to enforce the convergence

$$\frac{P(s)}{s + M(s)} G(s) \rightarrow \frac{M(s)}{s + M(s)} \tag{84}$$

This implies $G(s) \rightarrow M(s)/P(s)$, as required. The system switches to state 2 when a suitable measure of e(t) is sufficiently small. The feedforward and feedback copies $G_c(s)$ of G(s) are connected so that the actual control loop is closed. The closed-loop transfer function is

$$T(s) = G_c(s) \frac{P(s)}{s + M(s)} \simeq \frac{M(s)}{s + M(s)} = T_R(s) \tag{84}$$

The design concept shown in figure 10 will be referred to in the sequel as configuration 3. The advantage of this method, besides its simplicity, is that no direct plant identification is involved. The significance is that only fixed and normally well-damped modes of the model M(s) are involved, and the otherwise stringent requirements of high LMS filter fidelity often needed in the explcit identification of lightly damped plant modes are avoided. In practice, G(p) denoted by equation (2) and $G_c(p)$ denoted by equation (5) can be combined as a single filter.

COMPUTER SIMULATION TESTS

Outline

It is the purpose of the simulation tests described in this section to experimentally validate the design concepts of configurations 1, 2, and 3 as described in the section on Computer Simulation Tests. The principal issues are (1) the convergence processes of the parameter vectors $\underline{w}$ in plant or in controller identification; (2) the effects of parameter noise $\tilde{\underline{w}}$ and additive noise n; (3) the

precision with which the adapting system converges to the desired reference model $T_R(s)$; and (4) the suppression of lightly damped modes.

In the actual modeling, a principal issue has been to limit the number of varying parameters to the bare minimum without substantially sacrificing insights. To that end, the following steps were taken:

1. The reference model $T_R(s)$ given in equation (70)

$$T_R(s) = \frac{10}{s^3 + 6.5s^2 + 9s + 10}$$

was used in all the simulation tests.

2. In all the tests the excitation signal was white noise except for one case in which a band-limited excitation signal was applied for the purpose of comparison.

3. The principal filter parameters in all cases were chosen as $N = 60$, $\Delta T = 0.1$ sec.

4. In all cases the plant, reference models, and various system and noise filters were modeled in continuous time. Fourth-order Runge-Kutta integration was used and integration step size was $dT = 0.02$ sec.

5. In all cases the model of the plant was of the form

$$P(s) = \frac{(\omega_p/\alpha)(s + \alpha\omega_p)}{s^2 + 2\omega_p\zeta_p s + \omega_p^2}$$

The natural frequency was set to $\omega_p = 5$ sec^{-1} in all cases with the exception of one in which ω_p was set to $\omega_p = 25$ sec^{-1}. The damping coefficient ζ_p was varied between 0.001 and 1. By varying α, the location of the numerator zero was changed without affecting the DC gain of $P(s)$. For $1/\alpha = 0$, the relative degree of $P(s)$ is 2. For $1/\alpha > 0$ the relative degree is 1. For $\zeta_p = 1$ and $\alpha = 1$, $P(s)$ reduces to a first-order lag $P(s) = \omega_p/(s + \omega_p)$. Thus, by varying the two parameters α and ζ_p, a wide variation in plant dynamics and relative degree is covered.

For the sake of brevity, only the principal results of the simulation test are presented. These are (1) computed IIR of the plant or controller; (2) estimated FIR of the plant or controller; (3) convergence history of weights of the controller; and (4) step response of the reference model $T_R(s)$ along with the step response of the adapted closed-loop system.

In two cases a complete set of simulation results is given. They include in addition to the above, the time-history of the reference model, the controller, and the closed-loop system outputs.

Typically, simulation runs spanned over 3000 or 4000 iterations. As seen from the time-histories, these were by far in excess of the actual number of iterations needed for conditioning and adaptation.

Simulation Procedure

All simulation runs started with initial conditions set at zero for both the weight vectors $\underline{w}$ and the state variables of the dynamical system. In each run the first half was dedicated to the conditioning of the controller and the second half to the convergence of the adaptive control system. At the end of each run, the final value of the weight vector was written to file as "frozen weights" constituting the adapted controller.

In a second test run, which provides the step response of the adapted closed-loop control system, the frozen weights were read into the program.

Nomenclature in Simulation Plots

Simulation results are grouped under configurations 1, 2, and 3. For easy identification of variables and parameters, reference should be made to figures 8, 9, and 10, respectively, in which each self-adjusting filter is indicated by a slanting arrow and each filter is designated by a number (1) to (9) in accordance with the appropriate configuration. The output of each self-adjusting filter is marked by YF1, YF2, etc. The weights of each filter are indexed accordingly, e.g., w1(J), w2(J), etc., and they represent the appropriate FIR forms plotted in continuous line format. Time histories of weights are shown for a few selected weights. For example, w2(5), w2(10), and w2(30) describe the 5th, 10th, and 30th weight as a function of time. In the step responses of $T_R(s)$ and the adapted system, z_s is the adapted closed-loop system step response and z_m is the step response of $T_R(s)$.

Simulation Results

The principal parameters and data of the simulation presented here are listed in table I. The σ_i and σ_n symbols are the rms values of $i(t)$ and $n(t)$, respectively. Unless otherwise specified, they are white noise. The adaptation gain factors, F, in the identification loops and controller adjustment loops described in configurations 1 and 2 are represented by F_i and F_a (figs. 8 and 9). In configuration 3 (fig. 10) only one value of F is appropriate. The values of F_i and F_a are relatively small so that substantial parameter noise is present. The choice of $F_i = 6$, $F_a = 8$ is a compromise between precision of the estimates and

convergence time. Note that the choice $\Delta T = 0.1$ sec scales all FIR estimates by 1/10 (see appendix A).

Figure 11(a) (compare to fig. 12(a)) demonstrates good precision in the estimate of $P(s)/[s + M(s)]$; figure 11(b) shows a noisier estimate of $P(s)$ and figure 11(c), a still noisier estimate of the controller $G(s)$. This is to be expected since the three-stage estimation process of figure 8 causes cumulative weight noise in figures 11(a)-11(e). In spite of this weight noise, the adapted system step response z_s shown in figure 11(f) compares well with z_m.

Figure 12 describes the adaptation process including additive output noise with a noise-to-signal ratio of 0.05. To smooth the parameter noise, F_i and F_a were increased to 20 and the number of iterations was doubled. Figures 12(a) and 12(b) show unbiased, though somewhat noisy, estimates of $P(s)/[s + M(s)]$. Figure 12(c) shows the convergence history of $\bar{w}$ in $G(s)$. Figure 12(e) demonstrates similarity to the computed IIR in figure 12(d). However, because of limited fidelity the initial spikes are attenuated. The step response of the adapted system, shown in figure 12(c), though unbiased, is somewhat distorted. However, if $n(t)$ represents measurement noise, the example value of 0.05 for noise-to-signal ratio is quite high. Realistic noise-to-signal ratios are an order of magnitude smaller.

Figure 13(b) demonstrates an excellent estimate of $P(s)/[s + M(s)]$ (compare with fig. 13(a)). Figure 13(c) demonstrates a smooth transition from the training phase to the closed-loop adaptation phase which occurred at $t = 40$ sec. Figure 13(d) demonstrates relatively rapid convergence of the controller $G(s)$. Figure 13(e) shows that the controller estimate is noisy, yet the adapted closed-loop step response shown in figure 13(f) is quite close to that of the reference model.

Figure 14 demonstrates similar performance for the extreme case of $\alpha = 1$, or reduction to a first-order lag.

Figure 15(b), compared to fig. 15(a), demonstrates a good estimate of $G(s)$ even though $i(t)$ is band-limited to approximately 4 rad/sec. Figure 15(c) shows the actual time of convergence of the controller weights. Figure 15(d) demonstrates an excellent fit of the controller output YF2 and the reference model output XL (refer to fig. 10). Figure 15(e) describes the adapting plant output Z. The first 30 sec of the training phase show a relatively undamped response since the system is open loop. The last 30 sec, representing the actual adaptation phase, show the expected smoothed response. Figure 15(f) demonstrates an excellent fit between the step response of the adapted system and the reference model. Since only a one-stage estimation process is involved, the effect of parameter noise is quite small.

Figure 16 demonstrates similar behavior for a very lightly damped system. The estimated FIR of $G(s)$ in figure 16(b) is close to the corresponding IIR shown in figure 16(a). However, the limited filter fidelity attenuates the initial positive and negative spikes. The convergence process shown in figures 16(c), 16(d), and 16(e) demonstrates rapid conditioning and smooth transition to the adaptation

phase occurring at t = 30 sec and the gradual suppression of these modes in the last 30 sec. Figure 16(f) again shows excellent adapted step response.

Figure 17 shows a similar performance to that shown in figure 16 except that the damping was higher and the relative degree was 1.

Figures 18(a) and 18(b) demonstrate that the same LMS filter operates efficiently for ω_p = 25 rad/sec. It demonstrates a good estimate of G(s) and excellent adapted closed-loop step response.

Figures 19(a) and 19(b) demonstrate excellent FIR estimation of G(s) even for a system with the extremely small damping factor ζ_p = 0.001. Again, figure 19(c) demonstrates good adapted-step response.

Figure 20 demonstrates the effect of additive noise on configuration 3. The FIR estimate of G(s) as shown in figure 20(a) is clearly biased (compare with fig. 12(b)). Figure 20(b), accordingly, shows a deteriorated adapted-step response.

The results demonstrate the following:

1. Configuration 1, though providing an unbiased controller estimate, is relatively noisy due to the three-stage identification process.

2. Configuration 2 provides a less noisy and unbiased controller estimate and represents a suitable design for a wide variety of applications with process and measurement noise.

3. Configuration 3 is the most precise and is suitable in a variety of applications with insignificant process noise.

4. The adaptive controller performs well under a wide variation of plant parameter variations.

5. Transition from training phase to adaptation phase is smooth provided a sufficient number of training iterations is provided.

CONCLUSIONS

The investigation presented in this paper leads to the conclusion that nonparametric adaptive control, implemented by LMS transversal filters, is feasible. In applications where process or measurement noise is insignificant in comparison with the excitation signal, configuration 3 is superior. Since only a one-stage controller estimation process is involved, the weight noise is small and excellent convergence to the reference model is achieved. Because of the integral control, DC offsets do not cause bias in the controller. Furthermore, since no explicit plant identification is involved, the design of the single self-adjusting filter is primarily determined by the fixed eigenvalues of the reference model. Variations in the plant eigenvalues are reflected only as variations in controller zeros which do

not affect the filter quality in the sense of truncation error or fidelity. Large variations in plant zeros, however, can affect filter quality.

In applications with appreciable process noise, configuration 2 is preferable since noise-induced bias is prevented by the two-stage identification process. The resulting penalty of additional weight noise can be traded off against convergence-time by decreasing the adaptation coefficient 1/F. In numerous applications where parameter variations are slow or piecewise constant, the increased convergence time can be tolerated and considered as part of the training or conditioning period. Residual weight noise is largely suppressed by the closed-loop control system as evidenced by the real-time simulations described. The effective suppression of lightly damped modes demonstrated, points to promising applications in controlling unmodeled high-frequency modes and fine-tuning adaptive systems. The nonparametric nature of the FIR identification indicates that the method is equally applicable to lumped parameter or distributed systems.

APPENDIX A

PRINCIPLE OF OPERATION OF THE LMS FILTER

The basic structure of the transversal LMS filter is shown in figure A1 (for greater detail see references 4 and 5). With the sampler at its input $x(t)$, it represents a discrete implementation.

The real-time stationary input signal $x(t)$ is sampled and operated on by a set of linear operators, $f_1, f_2, \ldots, f_N$, which generate the vector $\underline{x}_j = [x_{1j}, x_{2j}, \ldots, x_{Nj}]^T$ at the discrete time-instances that are indexed by j. The components of $\underline{x}_j$ are assumed to constitute a linearly independent set. On weighting $\underline{x}_j^T$ by $\underline{w} \triangleq [w_1, w_2, \ldots, w_N]^T$ and combining the weighted component functions, the output $y_j = \underline{x}_j^T \underline{w}$ is generated. The squared error $e_j^2 = (d_j - y_j)^2$ determines the quadratic criterion function, where d_j is the desired output. The global convergence and stability properties of the basic LMS algorithm are best understood by taking the expectation $E[e_j^2]$. Thus,

$$\begin{aligned} E[e_j^2] &= E[d_j^2] - 2E[d_j \underline{x}_j^T]\underline{w} + \underline{w}^T E[\underline{x}_j \underline{x}_j^T]\underline{w} \\ &= E[d_j^2] - 2\underline{P}^T \underline{w} + \underline{w}^T R \underline{w} \end{aligned} \tag{A1}$$

where

$$\underline{P} \triangleq E[d_j \underline{x}_j] = E\begin{bmatrix} d_j x_{1j} \\ \\ d_j x_{Nj} \end{bmatrix} \tag{A2}$$

$$R = E[\underline{x}_j \underline{x}_j^T] = E\begin{bmatrix} x_{1j}x_{1j} & \cdots & x_{1j}x_{Nj} \\ \vdots & & \vdots \\ x_{Nj}x_{1j} & \cdots & x_{Nj}x_{Nj} \end{bmatrix} \tag{A3}$$

Equation (A1) is a quadratic form in the parameter space $\{\underline{w}\}$. We seek to minimize $E[e_j^2]$ and apply a gradient, or steepest-descent algorithm. The ensemble averaged gradient is

$$\underline{\nabla}_j = \partial[E(e_j^2)]/\partial \underline{w}\Big|_{\underline{w}=\underline{w}_j} = \begin{bmatrix} \partial E(e_j^2)/\partial w_1 \\ \\ \partial E(e_j^2)/\partial w_N \end{bmatrix}_{\underline{w}=\underline{w}_j} = -2\underline{P} + 2R\underline{w}_j \tag{A4}$$

Setting $\underline{\nabla}_j = 0$, the solution for $\underline{w}$ is $\underline{w}^*$;

$$\underline{w}^* = R^{-1}\underline{P} \tag{A5}$$

The index j is dropped since $\nabla_j = 0$ implies the asymptotic value of $\underline{w}_j$. The steepest-descent algorithm is

$$\Delta \underline{w}_j = \underline{w}_{j+1} - w_j = -\mu \underline{\nabla}_j \tag{A6}$$

where μ is a constant coefficient. Explicitly,

$$\Delta \underline{w}_j = -\mu[-2\underline{P} + 2R\underline{w}_j] = -2\mu R\underline{w}_j + 2\mu\underline{P} \tag{A7}$$

Equation (A7) is a linear difference vector equation.

Since R is a real symmetric and a nonnegative definite matrix, all its eigenvalues have nonnegative real parts and $\Delta \underline{w}_j$ constitutes a globally asymptotically stable process which converges to the optimum Wiener solution uniquely defined by equation (A5) provided that the gain μ is sufficiently small.

The real-time implementation of the LMS algorithm is accomplished by directly minimizing e_j^2, through

$$\hat{\underline{\nabla}}_j = \frac{\partial}{\partial \underline{w}} e_j^2\Big|_{\underline{w}=\underline{w}_j} \tag{A8}$$

which is shown to be realizable through the relation

$$\hat{\underline{\nabla}}_j = \frac{\partial}{\partial \underline{w}} e_j^2\Big|_{\underline{w}=\underline{w}_j} = 2e_j \frac{\partial e_j}{\partial \underline{w}}\Big|_{\underline{w}=\underline{w}_j} \tag{A9}$$

Since

$$e_j = d_j - \underline{x}_j^T \underline{w}_j \tag{A10}$$

is a linear error equation in $\underline{w}_j$,

$$\left.\frac{\partial e_j}{\partial \underline{w}}\right|_{\underline{w}=\underline{w}_j} = -\underline{x}_j \tag{A11}$$

where e_j and $\underline{x}_j$ are both realizable variables (fig. A1), and the instantaneous gradient $\hat{\underline{\nabla}}_j$ in equation (A9) is realizable. Thus, the necessary conditions for implementing the LMS algorithm are (1) realizability of the input derived vector $\underline{x}_j$, and (2) realizability of $\partial e_j/\partial \underline{w}_j$ and its independence of $\underline{w}_j$ thus assuring the linearity of equation (A10).

From equations (A6), (A9), and (A11) we have

$$\underline{w}_{j+1} = \underline{w}_j - \mu\hat{\underline{\nabla}}_j = \underline{w}_j + 2\mu e_j\underline{x}_j \tag{A12}$$

To ensure stable convergence of equation (A12), the step sizes $\mu\hat{\underline{\nabla}}_j$ must be chosen so that they are sufficiently small. It can be shown (ref. 5) that the sufficient condition is

$$0 < \mu < 1/\lambda max \tag{A13}$$

where λmax is the largest eigenvalue of the covariance matrix R. λmax is difficult to estimate; therefore, equation (A13) is replaced by

$$0 < \mu < 1/trR \tag{A14}$$

Since $trR \geq \lambda max$, equation (A14) is more conservative than equation (A13) thus ensuring stability. The advantage of equation (A14) is that trR can be estimated on line and used to determine μ.

The process of convergence of the LMS filter follows, on the average, an exponential law. It can be shown (ref. 5) to have an equivalent time-constant

$$\tau_{it} \approx N/4\mu trR \tag{A15}$$

where τ_{it} is measured in the number of steps j, and N is the number of weights. Specifically, if f_k $(k = 1, \ldots, N - 1)$ is $f_k = \Delta$ for k and Δ is a pure time-delay one has

$$x_{kj} = x_j\Delta^{k-1} = x(j - k + 1) \tag{A16}$$

and

$$y_j = \sum_{k=1}^{N} y_{kj} = \sum_{k=1}^{N} w_{kj}x(j - k + 1) \tag{A17}$$

The components x_{kj}, $k = 1,N$ are obtained from a tapped delay line. Thus, the LMS filter assumes the explicit form of a convolution of $\underline{w}$ and $\underline{x}$ in which $\underline{w} \triangleq [w_1, w_2, \ldots, w_N]^T$ represents the discrete finite impulse response (FIR) of the filter. An additional factor which is involved in the choice of μ is the misadjustment M (ref. 5). It defines the excess parameter noise in $\underline{w}$ over the asymptotic Wiener solution. M is shown to be related to μ and R by

$$M = \mu \mathrm{tr} R \tag{A18}$$

Thus, for a given power level, subject to stable operation, M is proportional to μ. In accordance with equation (A14), we choose

$$\mu = 1/F\mathrm{tr}R \tag{A19}$$

where $F \geq 1$ ensures stability. Combining equations (A18) and (A19)

$$M = 1/F \tag{A20}$$

Thus, besides ensuring stability, the misadjustment can be determined through the design parameter F.

The roles of the input x(t) and the output d(t) are decided by the specific application and the position of the filter in a system.

To facilitate the description and analysis based on LMS-type self-adjusting filters, each individual filter will be represented in simplified format as indicated, e.g., in figure A2, where the role of the filter is to provide an estimate $\hat{P}$ of a plant P.

It should be noted that the estimated values w_{kj} are proportional to ΔT, i.e., the actual time increment between successive components x_{kj}, $x_{(k+1)j}$. Design considerations dictate the actual length T_f of the tapped delay line, $T_f = N\,\Delta T$.

Thus, for given T_f and ΔT, $N = T_f/\Delta T$. The values of x_{kj} are given by the input. Assume, for simplicity, $x_{kj} = C$ = constant and that w_k are all equal for a given duration $T = T_f$. Therefore,

$$y_j = C \sum_{k=1}^{N} w_k = CNw_k = CT_f \frac{w_k}{\Delta T}$$

Since y_j is independently dictated by $y_j \to d_j$, $w_k/\Delta T$ must be constant. Thus, in actual computer implementations of the LMS estimation process, the numerical values of w_k are proportional to ΔT.

APPENDIX B

EQUIVALENCE OF PROCESS AND MEASUREMENT NOISE IN PARAMETER ESTIMATION

Figure 4 describes a plant $P(p)$ in a closed loop, G represents the feedforward and feedback gains; $n(t)$ and $v(t)$ represent process and measurement noise, respectively. $\hat{P}(p)$ is an adjustable model of $P(p)$. The error $e(t)$ adjusts $\hat{P}(p)$ by means of a gradient algorithm. We consider the effect of $n(t)$ and $v(t)$ on the identification process.

It is easily verified that actual output $z(t)$ is given by

$$z(t) = \frac{GP(p)}{1 + GP(p)} [i(t) - v(t)] + \frac{1}{1 + GP(p)} n(t) \tag{B1}$$

$$z_m(t) = \frac{GP(p)}{1 + GP(p)} i(t) + \frac{1}{1 + GP(p)} [n(t) + v(t)] \tag{B2}$$

Thus, with respect to $z(t)$, $v(t)$ is equivalent to an input $i(t)$ while $n(t)$ is suppressed by the loop gain. With respect to $z_m(t)$, $v(t)$ and $n(t)$ are equivalent output disturbances.

It is also easily verified that

$$e(t) = \frac{G}{1 + GP(p)} [P(p) - \hat{P}(p)]i(t) + \frac{1 + G\hat{P}(p)}{1 + GP(p)} [n(t) + v(t)] \tag{B3}$$

It follows from equation (B3) that neither $n(t)$ nor $v(t)$ provides persistent excitation for the parameter estimation process since they are not common to $P(p)$ and $\hat{P}(p)$ as is $i(t)$.

The second term, because of $n(t) + v(t)$, causes biased estimates of $P(p)$. This is readily seen from the generic expression

$$\hat{P}(p) = -k \frac{\partial}{\partial \hat{P}(p)} e^2 = -2k\, e \frac{\partial e}{\partial \hat{P}(p)} \tag{B4}$$

From equation (B3) it is obvious that the product $e\partial e/\partial \hat{P}$ is proportional to $[n(t) + v(t)]^2$ which causes the biased estimate.

REFERENCES

1. Morse, A. S.: Global Stability of Parameter Adaptive Control Systems. IEEE Trans. on Automatic Control, vol. A-C 25, no. 3, June 1980, pp. 433-440.

2. Astrom, K. J.: Theory and Applications of Adaptive Control--A Survey. Automatica, vol. 19, no. 5, 1983, pp. 471-486.

3. Kreisselmeier, G.: On Adaptive State Estimation. IEEE Trans. on Automatic Control, vol. A-C 27, no. 1, Feb. 1982, pp. 3-17.

4. Widrow, B.; McCool, J. M.; Larimore, M. G.; and Johnson, C. R.: Stationary and Nonstationary Learning Characteristics of the LMS Adaptive Filter. Proc. IEEE, vol. 64, no. 8, Aug. 1976, pp. 1151-1162.

5. Widrow, B.; Glover, J. R.; McCool, J. M.; Kaunitz, J.; Williams, L. S.; Hearn, R. H.; Zeidler, J. R.; Dong, E.; and Goodlin, R. C.: Adaptive Noise Cancelling: Principles and Applications. Proc. IEEE, vol. 63, no. 12, Dec. 1975, pp. 1692-1716.

6. Friedlander, B.: Lattice Filters for Adaptive Processing. Proc. IEEE, vol. 70, no. 8, Aug. 1982, pp. 829-866.

7. Velger, M.; Grunwald, A.; and Merhav, S.: Suppression of Biodynamic Disturbances and Pilot Induced Oscillations by Adaptive Filtering. AIAA J. of Guidance and Control, vol. 7, no. 4, Aug. 1984, pp. 401-409.

8. Sundarajan, N.; Williams, J. P.; and Montgomery, R. C.: Adaptive Modal Control of Structural Dynamic Systems Using Recursive Lattice Filters. AIAA J. of Guidance and Control, vol. 8, no. 2, Apr. 1985, pp. 223-230.

9. Widrow, B.; McCool, J. M.; and Medoff, B. P.: Adaptive Control by Inverse Modeling. Stanford University Report, 1978.

10. Widrow, B.; Shur, D.; and Shaffer, S.: On Adaptive Inverse Control. Fifteenth Asilomar Conference on Circuits, Systems and Computers, Nov. 1981.

11. Widrow, B.; and Walach, E.: Adaptive Signal Processing for Adaptive Control. IFAC Workshop on Adaptive Systems in Control and Signal Processing, San Francisco, CA, June 1983.

TABLE 1.- PRINCIPAL PARAMETERS IN SIMULATION TESTS

Figure number	Configuration number	Iterations	Time, sec	σ_i	σ_n	F_i	F_a	Transfer function of P(s)	ω_p sec^{-1}	ζ_p	Comments
11	1	4000	80	20	0	6	8	$25/(s^2 + 2s + 25)$	5	0.2	
12	2	8000	160	20	1	20	20	$25/(s^2 + 2s + 25)$	5	.2	n(t) is white noise: noise/signal = 0.05
13	2	4000	80	20	0	6	8	$5(s + 5)/(s^2 + 2s + 25)$	5	.2	
14	2	4000	80	20	0	6	8	$5(s + 5)/(s^2 + 10s + 25)$	5	1	P(s) is reduced to $5/(s + 5)$
15	3	3000	60	20	0	6	--	$25/(s^2 + 1s + 25)$	5	.1	i(t) is second order band limited by filter $100/(s + 4)(s + 25)$
16	3	3000	60	20	0	6	--	$25/(s^2 + 0.1s + 25)$	5	.01	
17	3	3000	60	20	0	6	--	$5(s + 5)/(s^2 + 2s + 25)$	5	.2	
18	3	3000	60	20	0	6	--	$625/(s^2 + 5s + 625)$	25	.1	
19	3	3000	60	20	0	6	--	$5(s + 5)/(s^2 + 0.01s + 25)$	5	.001	
20	3	4000	80	20	1	20	--	$25/(s^2 + 2s + 25)$	5	.2	n(t) is white noise: noise/signal = 0.05

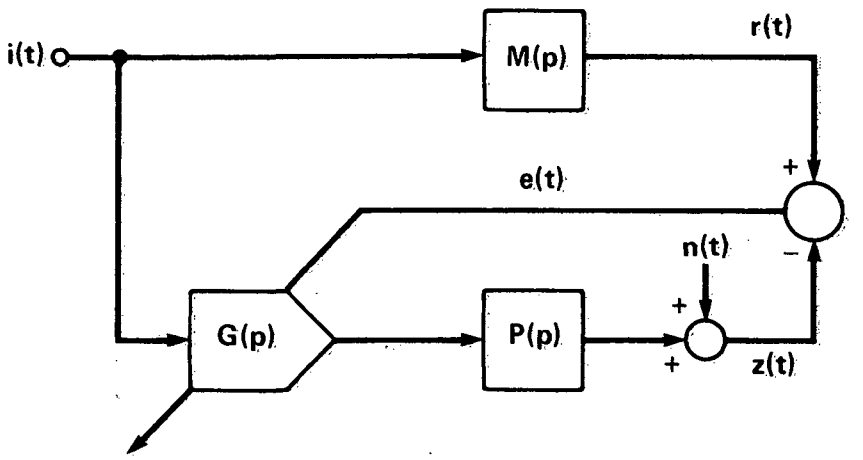

Figure 1.- Open-loop model reference adaptive control (improper configuration).

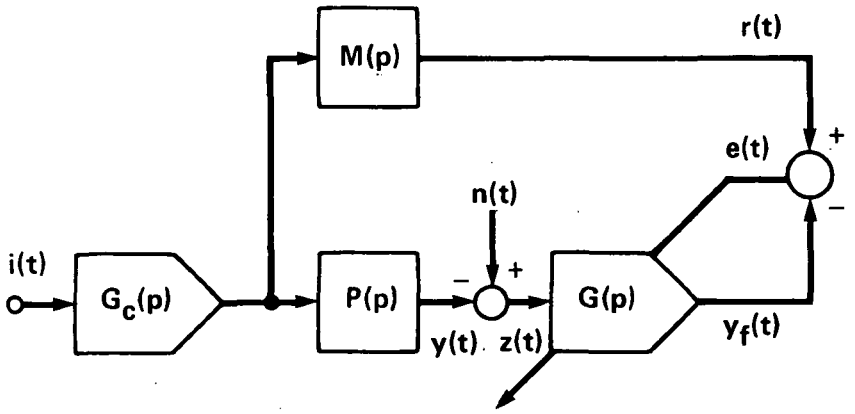

Figure 2.- Open-loop model reference adaptive control (proper configuration).

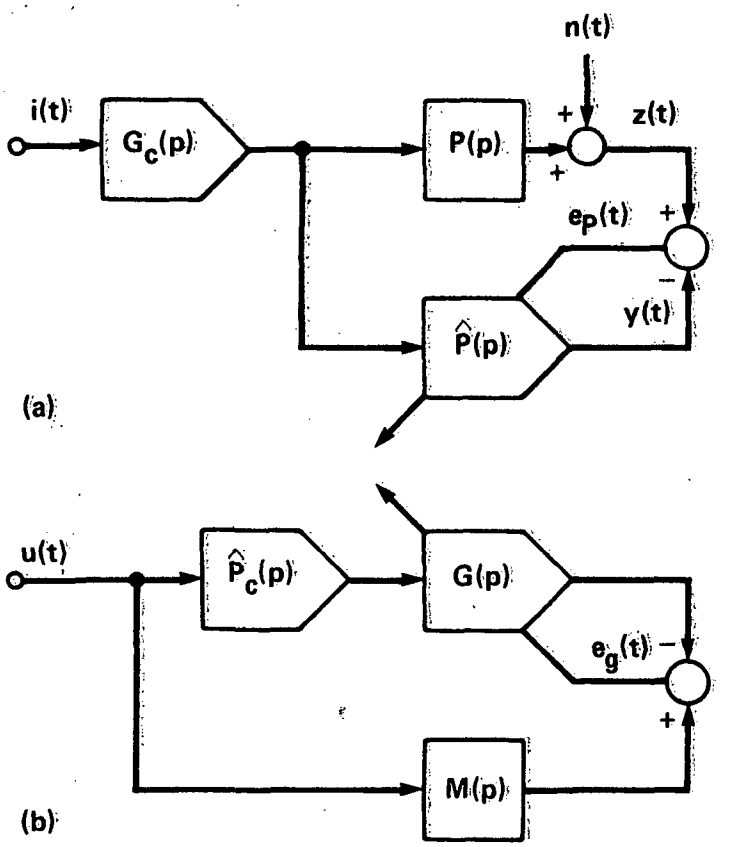

(a) Plant identification.

(b) Controller computation.

Figure 3.- Open-loop model reference adaptive control with explicit plant identification.

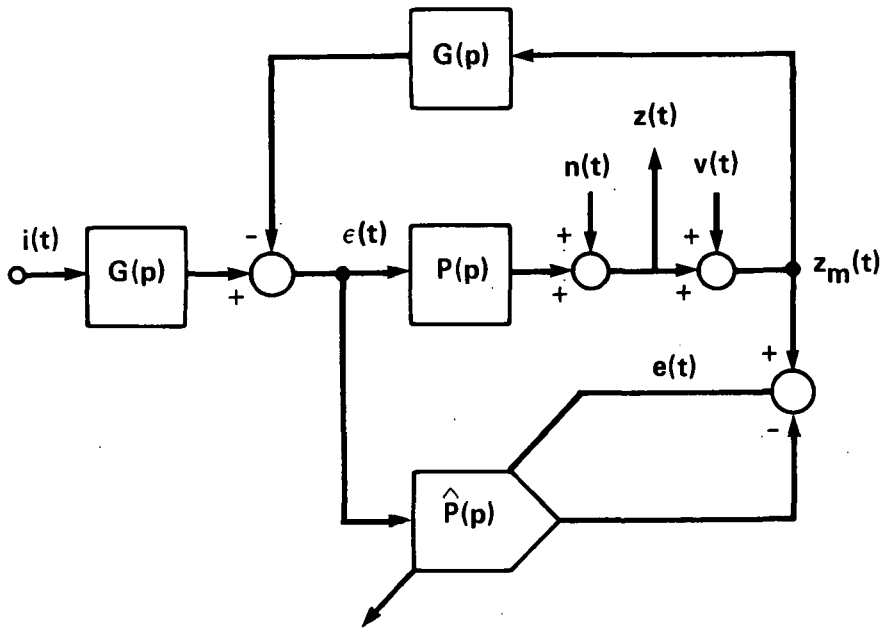

Figure 4.- Plant identification in a closed-loop system with process and measurement noise.

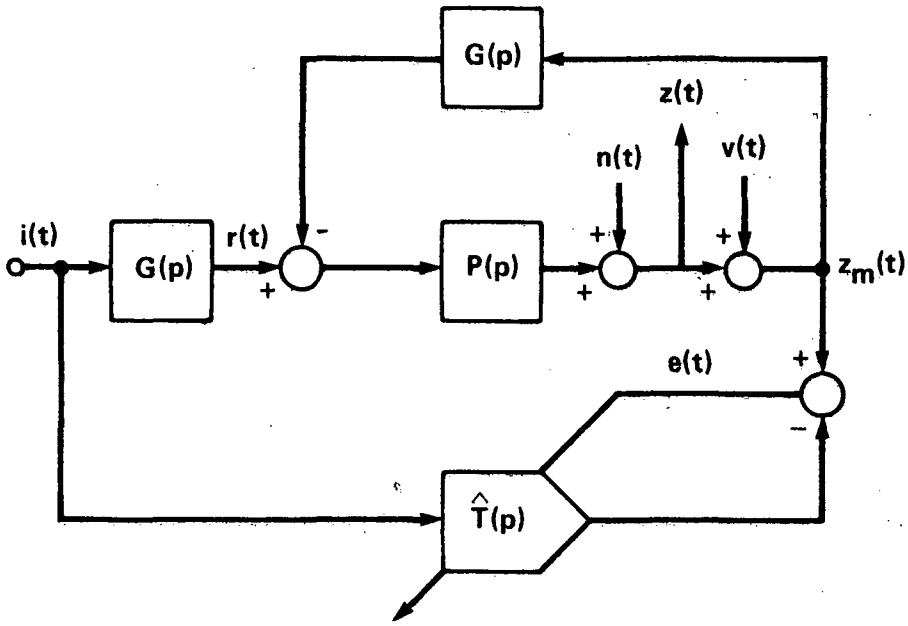

Figure 5.- Closed-loop system identification with process and measurement noise.

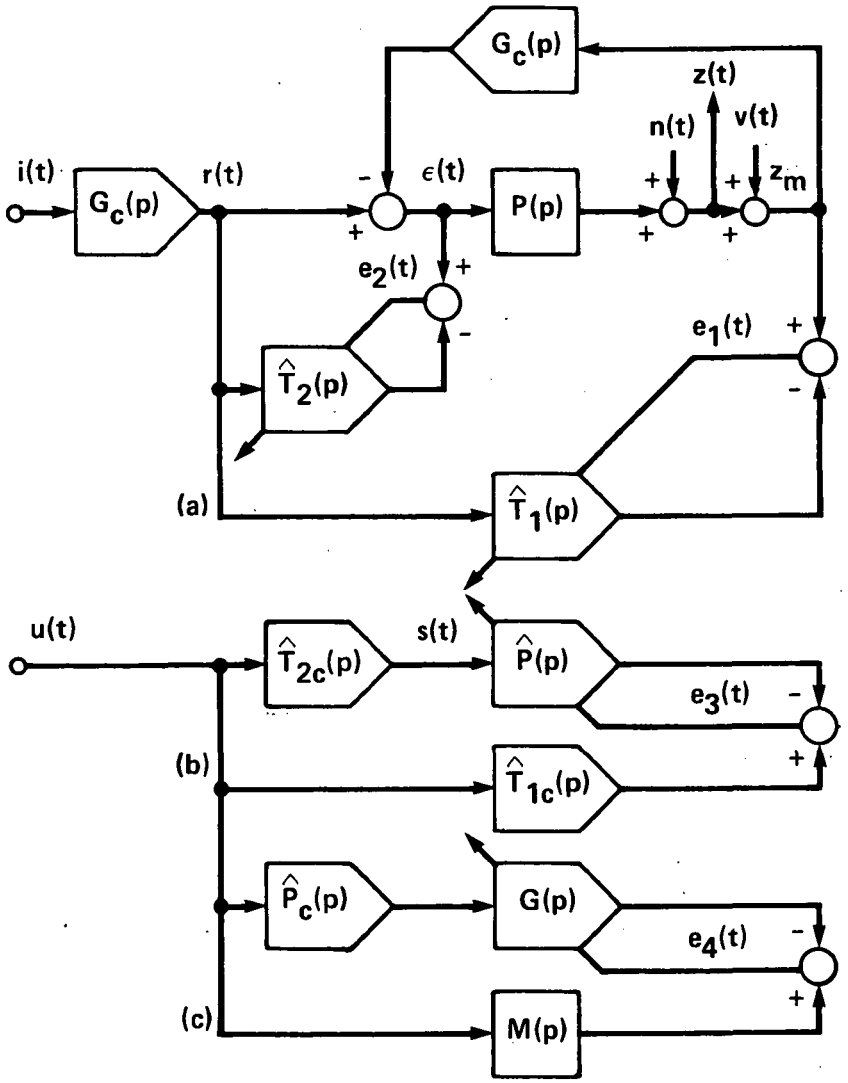

(a) Intermediate identification of $T_1(p)$ and $T_2(p)$.

(b) Identification of $P(p)$.

(c) Computation of $G(p)$.

Figure 6.- Two-stage explicit plant identification and MRAC controller computation--the indirect method.

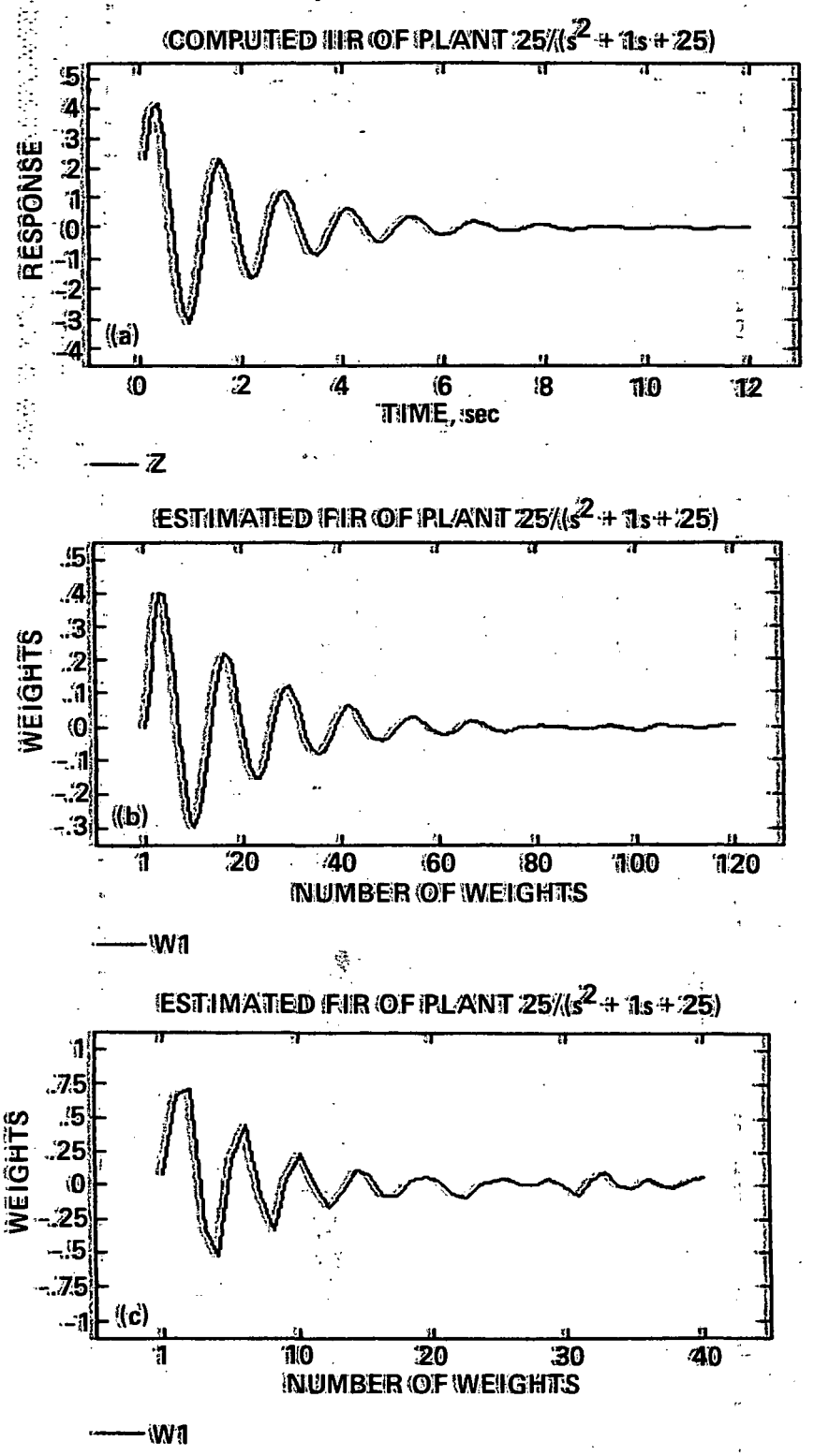

((a)) IIR of plant..

((b)) FIR for N = 120..

((c)) FIR for N = 40..

Figure 7.- Effect of the number of weights N on filter fidelity for a lightly damped plant..

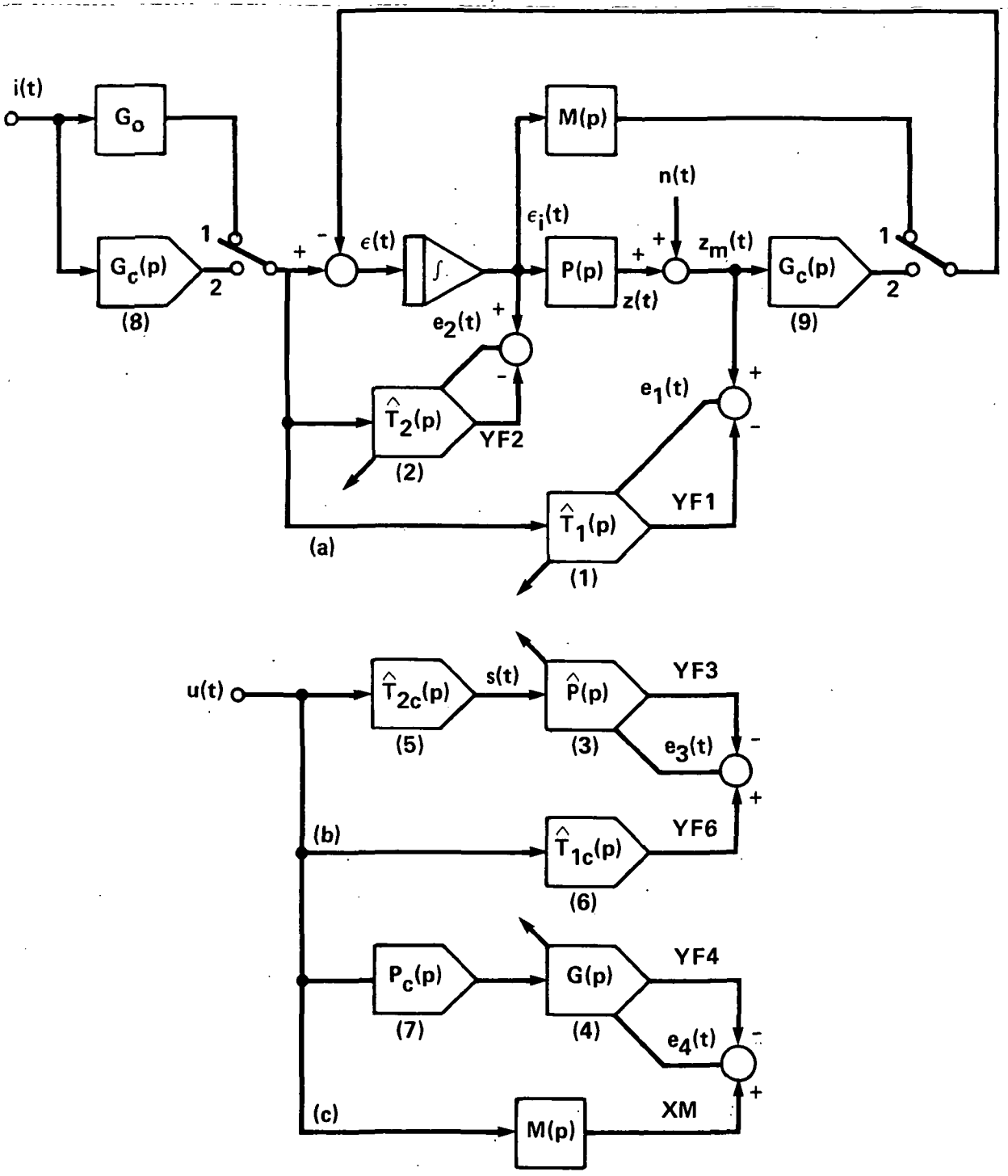

(a) Intermediate identification of $T_1(p)$ and $T_2(p)$.

(b) Identification of $P(p)$.

(c) Computation of $G(p)$.

Figure 8.- Implementation of MRAC, the indirect method; configuration 1.

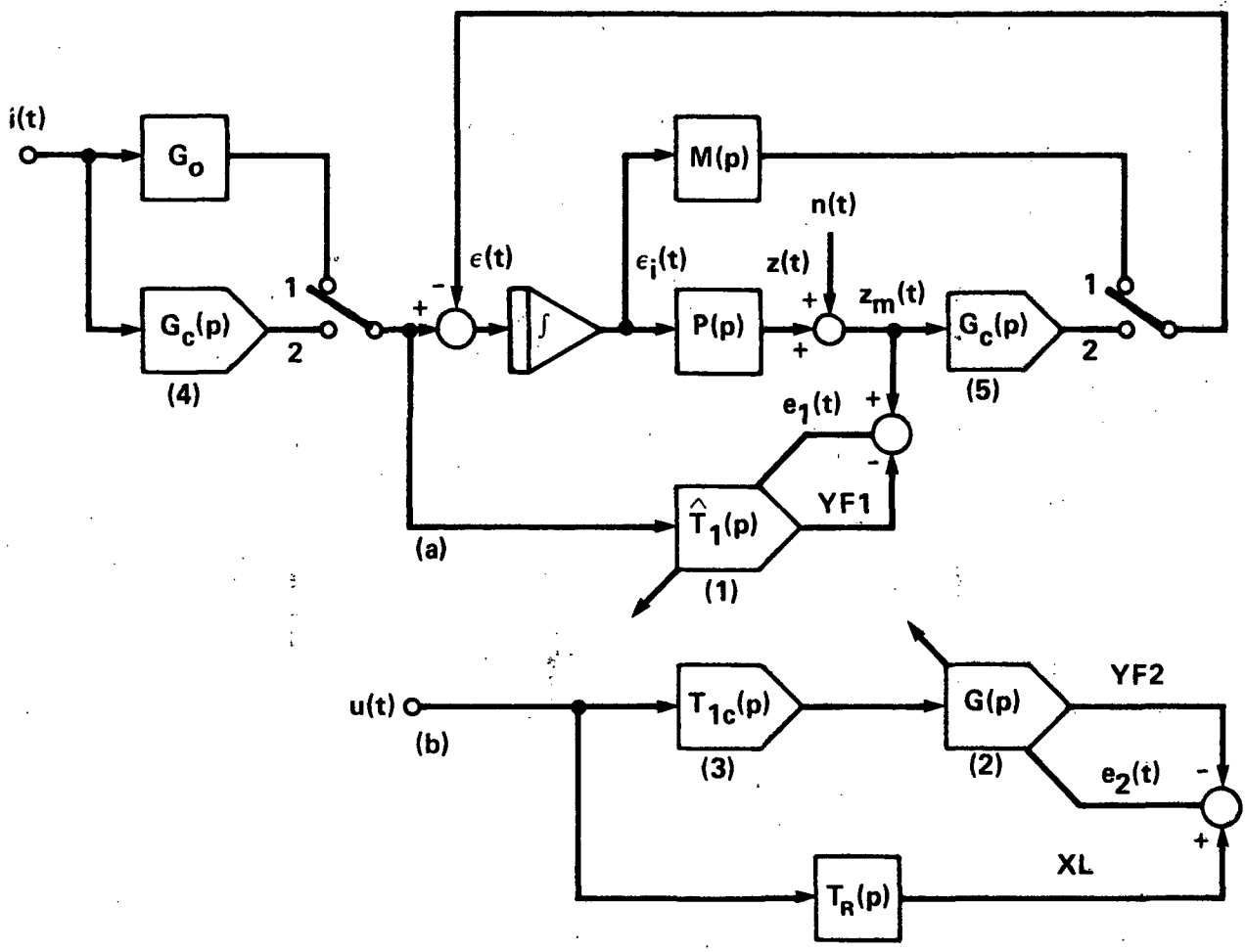

(a) Intermediate identification of $T_1(p)$.

(b) Computation of G(p).

Figure 9.- Implementation of MRAC, the indirect method; configuration 2.

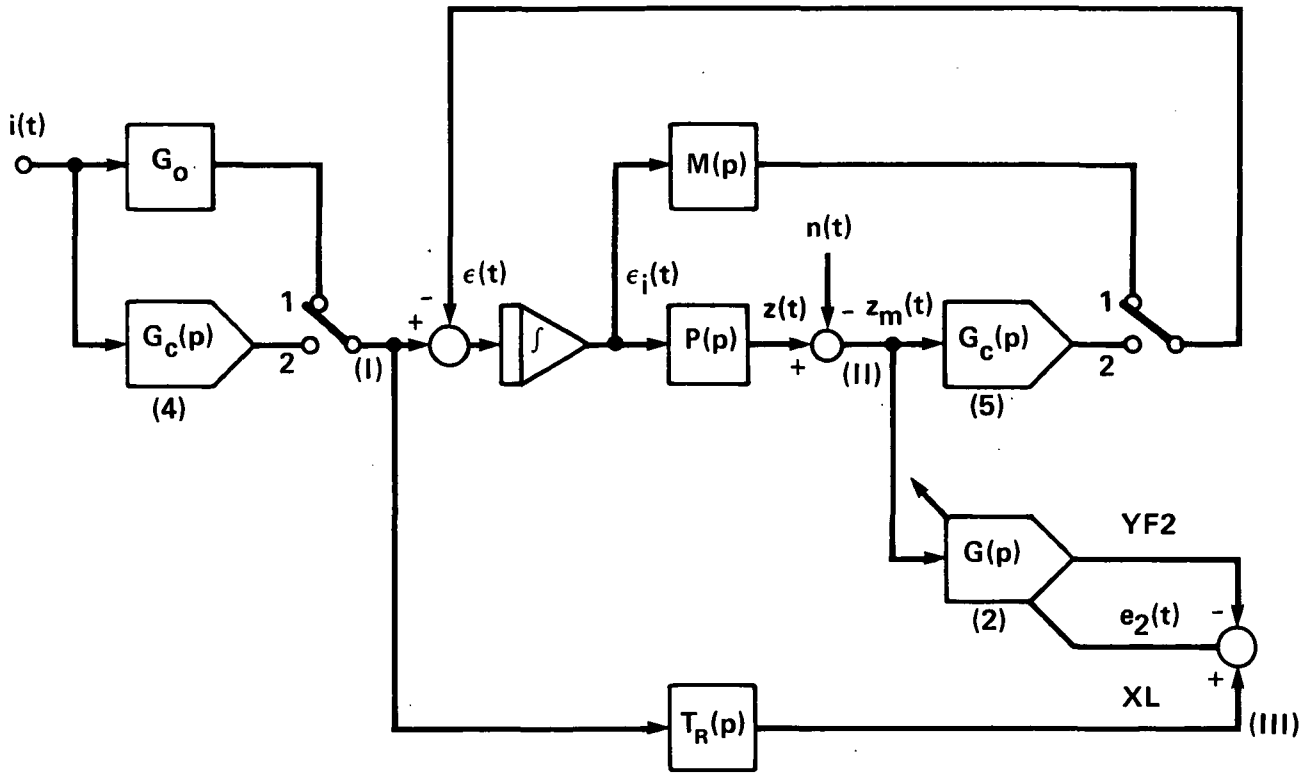

Figure 10.- Implementation of MRAC, the direct method; configuration 3.

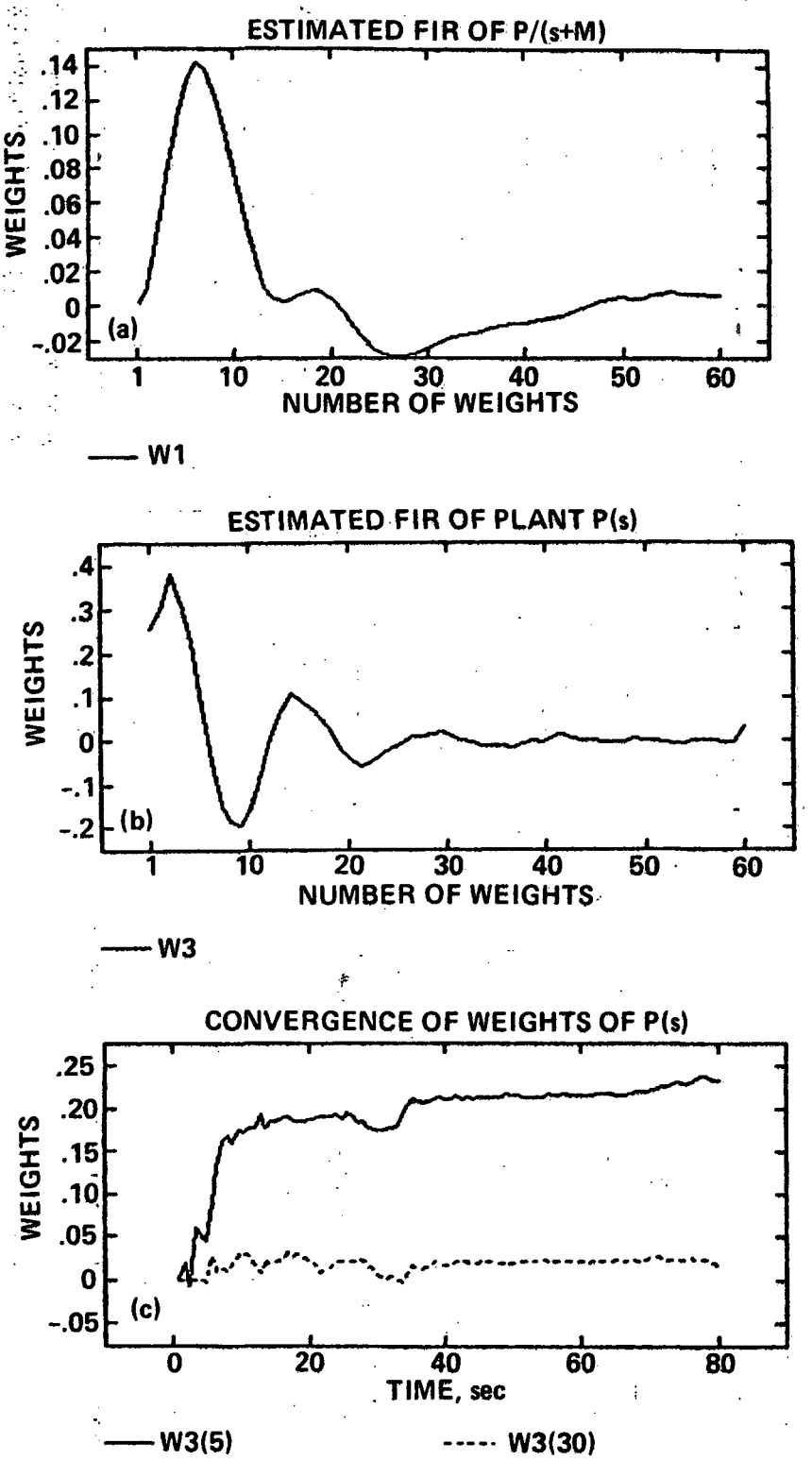

(a) Estimated FIR of $P/(s + M)$.

(b) Estimated FIR of $P(s)$.

(c) Convergence history of the weights of $P(s)$.

Figure 11.- Configuration 1, $P(s) = 25/(s^2 + 2s + 25)$.

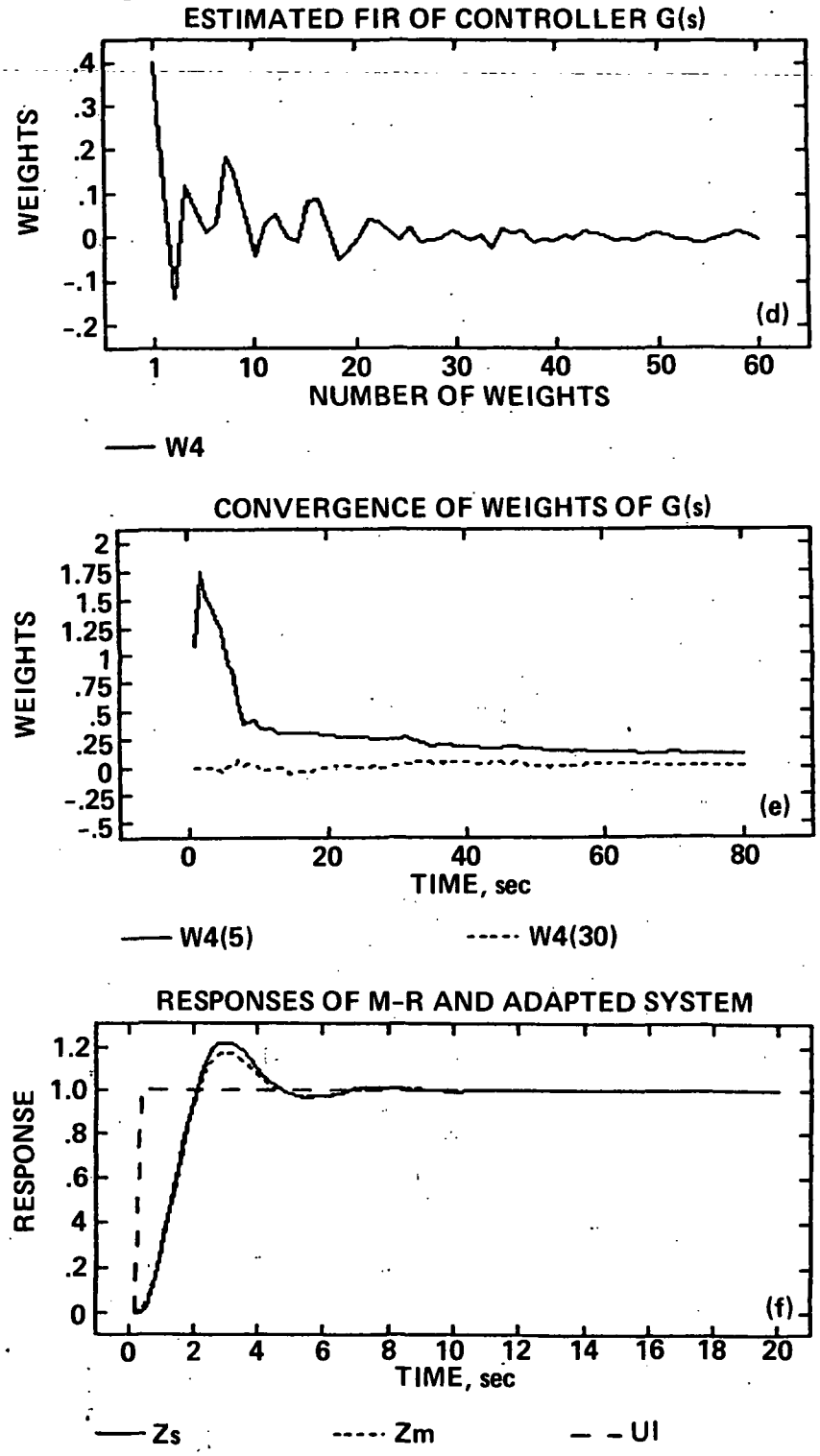

(d) Estimated FIR of controller G(s).

(e) Convergence history of the weights of G(s).

(f) Step responses of the reference model and the adapted system.

Figure 11.- Concluded.

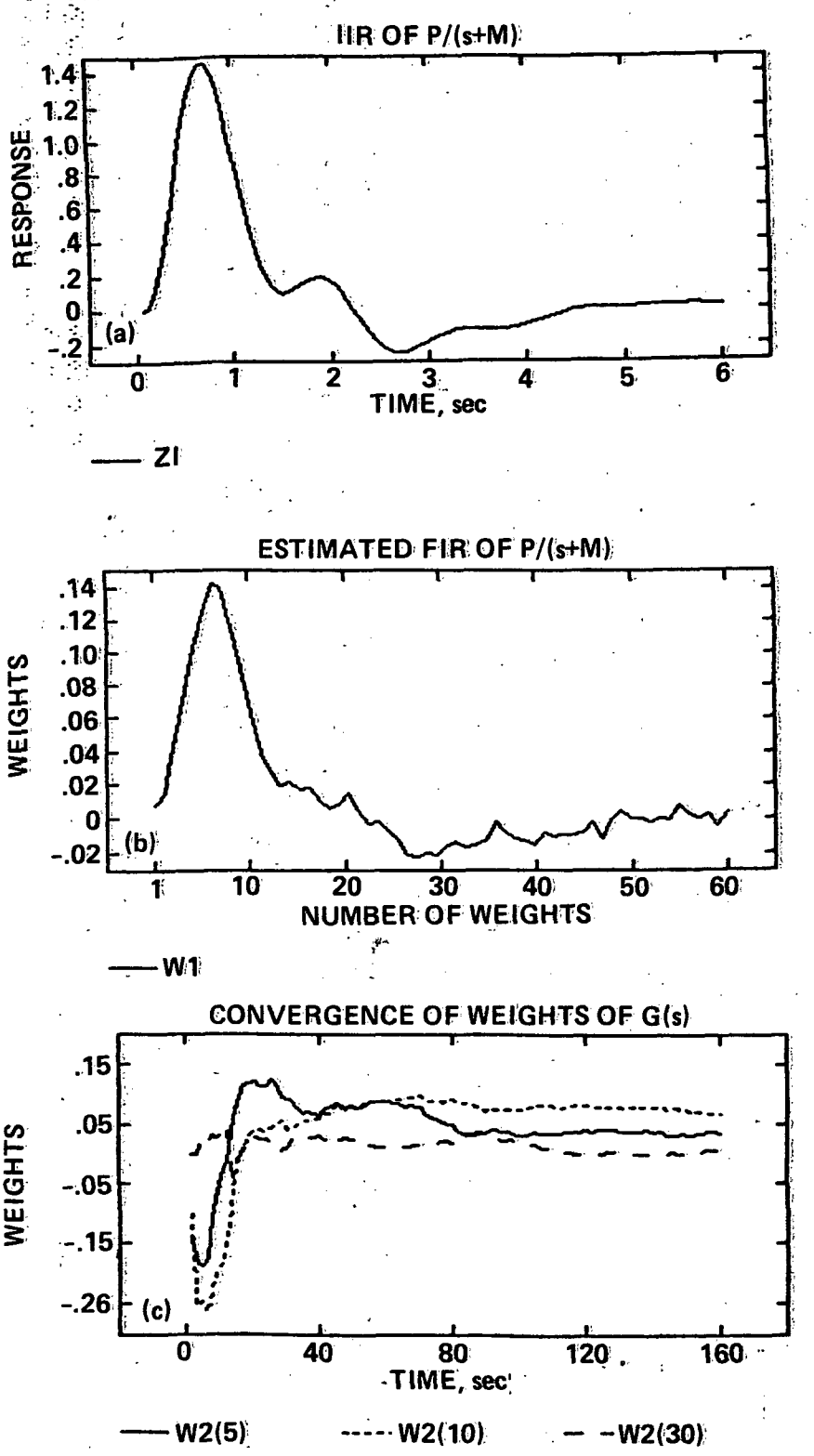

(a) Computed IIR of $P/(s + M)$.

(b) Estimated FIR of $P/(s + M)$.

(c) Convergence history of the weights of $G(s)$.

Figure 12.- Configuration 2, $P(s) = 25/(s^2 + 2s + 25)$; noise-to-signal ratio 0.05.

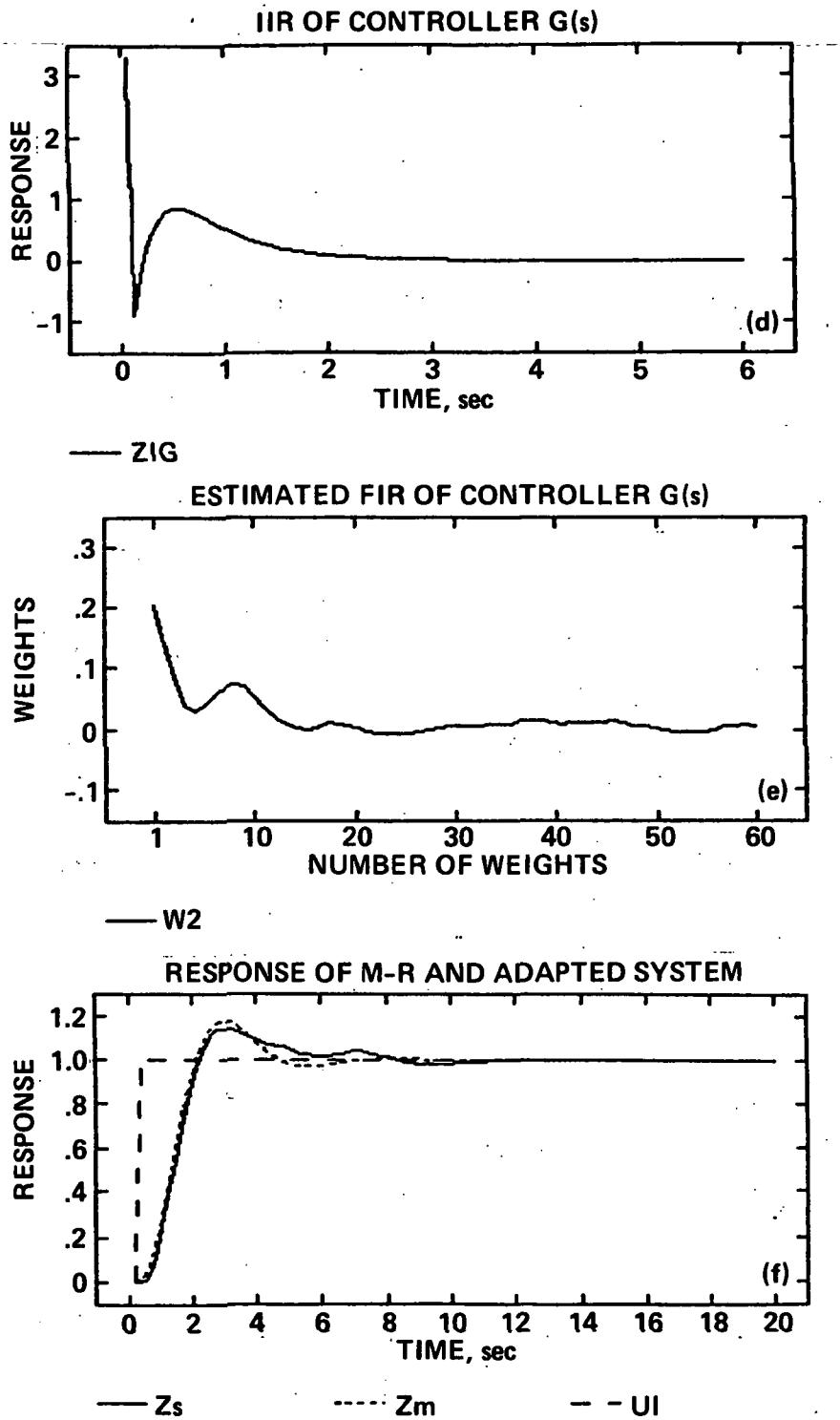

(d) Computed IIR of the controller G(s).

(e) Estimated FIR of the controller G(s).

(f) Step responses of the reference model and the adapted system.

Figure 12.- Concluded.

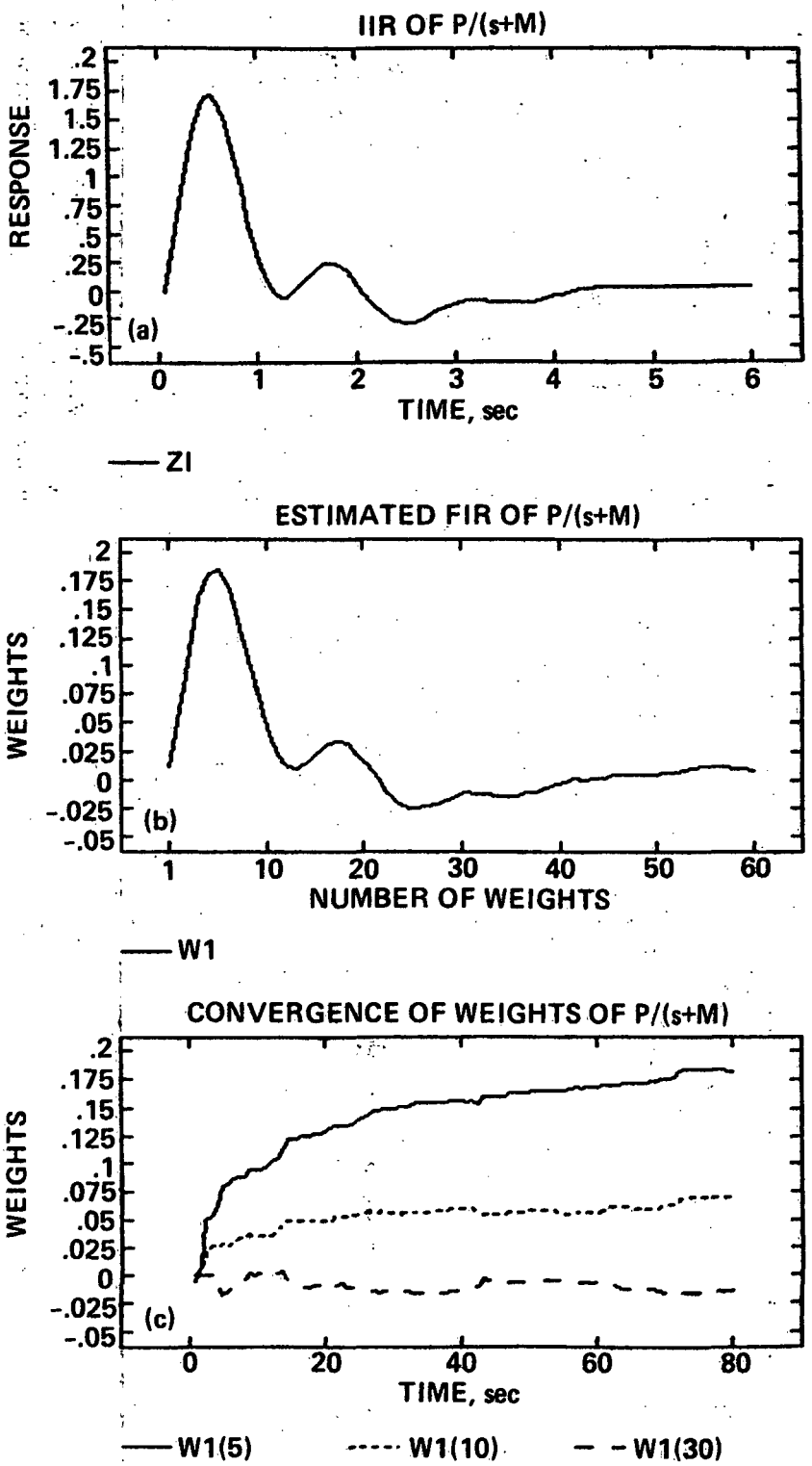

(a) Computed IIR of $P/(s + M)$.

(b) Estimated FIR of $P/(s + M)$.

(c) Convergence history of the weights of $P/(s + M)$.

Figure 13.- Configuration 2, $P(s) = 5(s + 5)/(s^2 + 2s + 25)$.

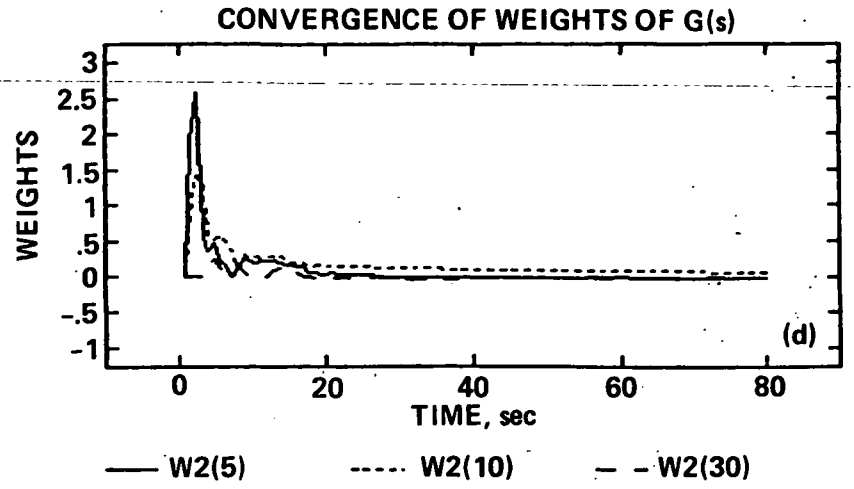

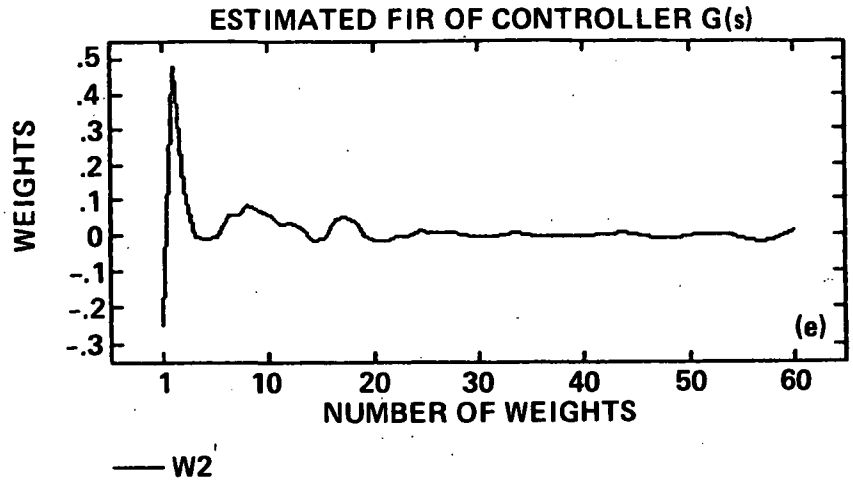

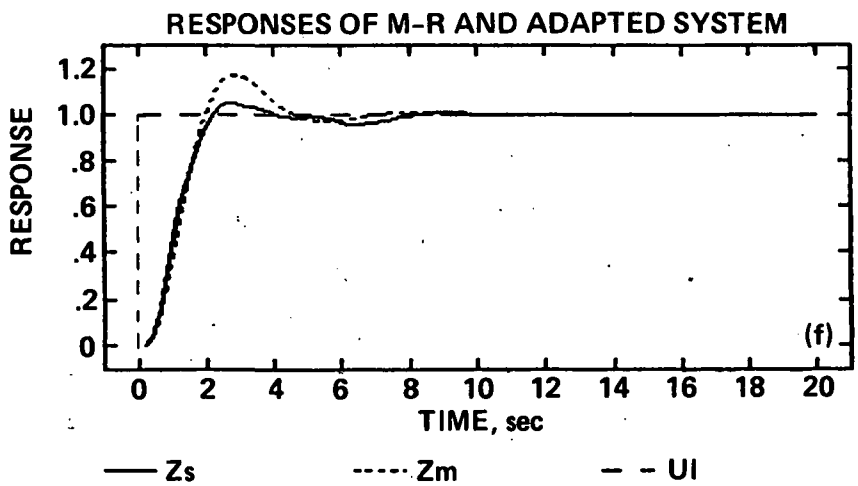

(d) Convergence history of the weights of G(s).

(e) Estimated FIR of the controller G(s).

(f) Step responses of the reference model and the adapted system.

Figure 13.- Concluded.

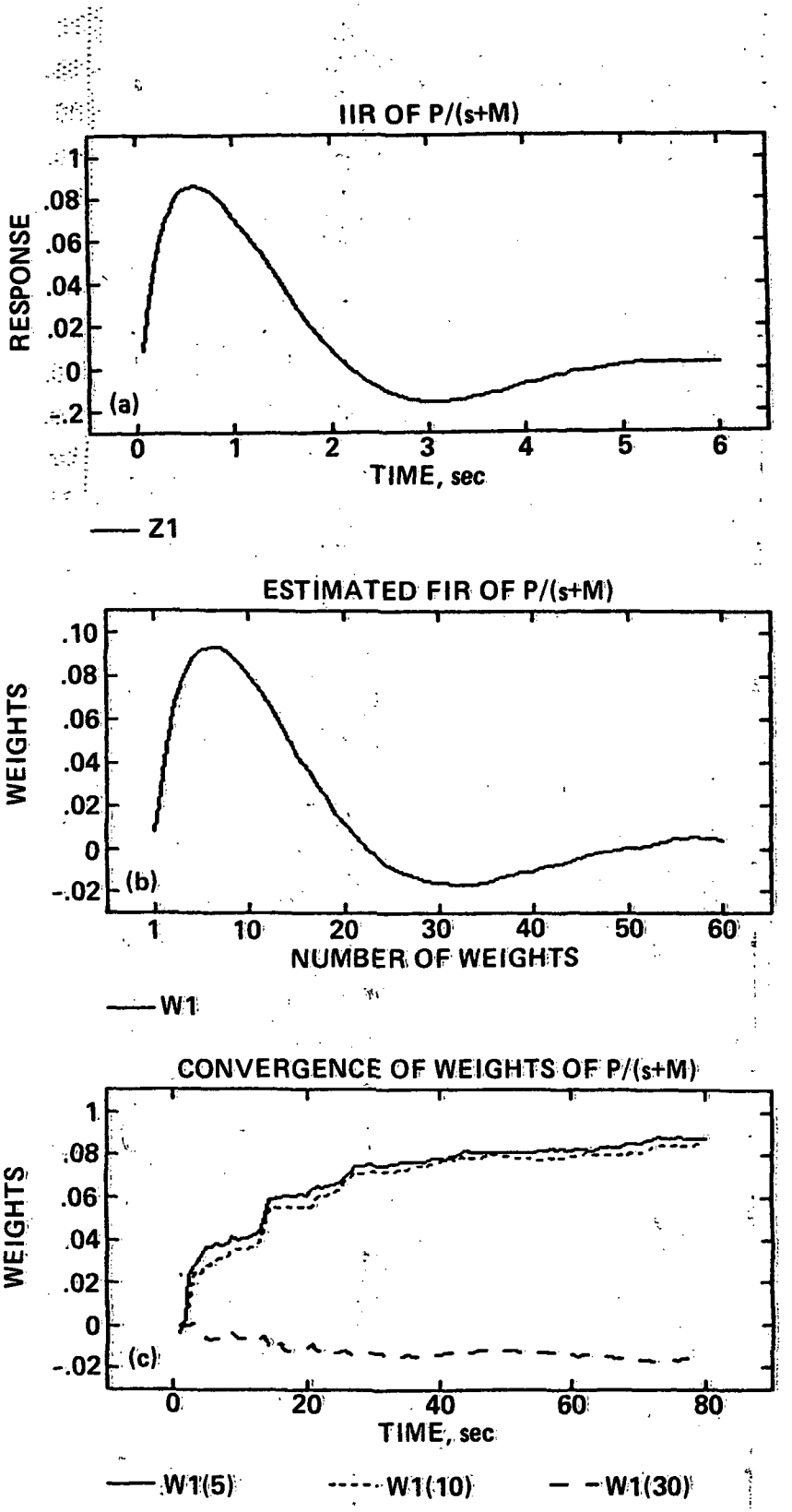

(a) Computed IIR of $P/(s + M)$.

(b) Estimated FIR of $P/(s + M)$.

(c) Convergence history of the weights of $P/(s + M)$.

Figure 14.- Configuration 2, $P(s) = 5(s + 5)/(s^2 + 10s + 25)$.

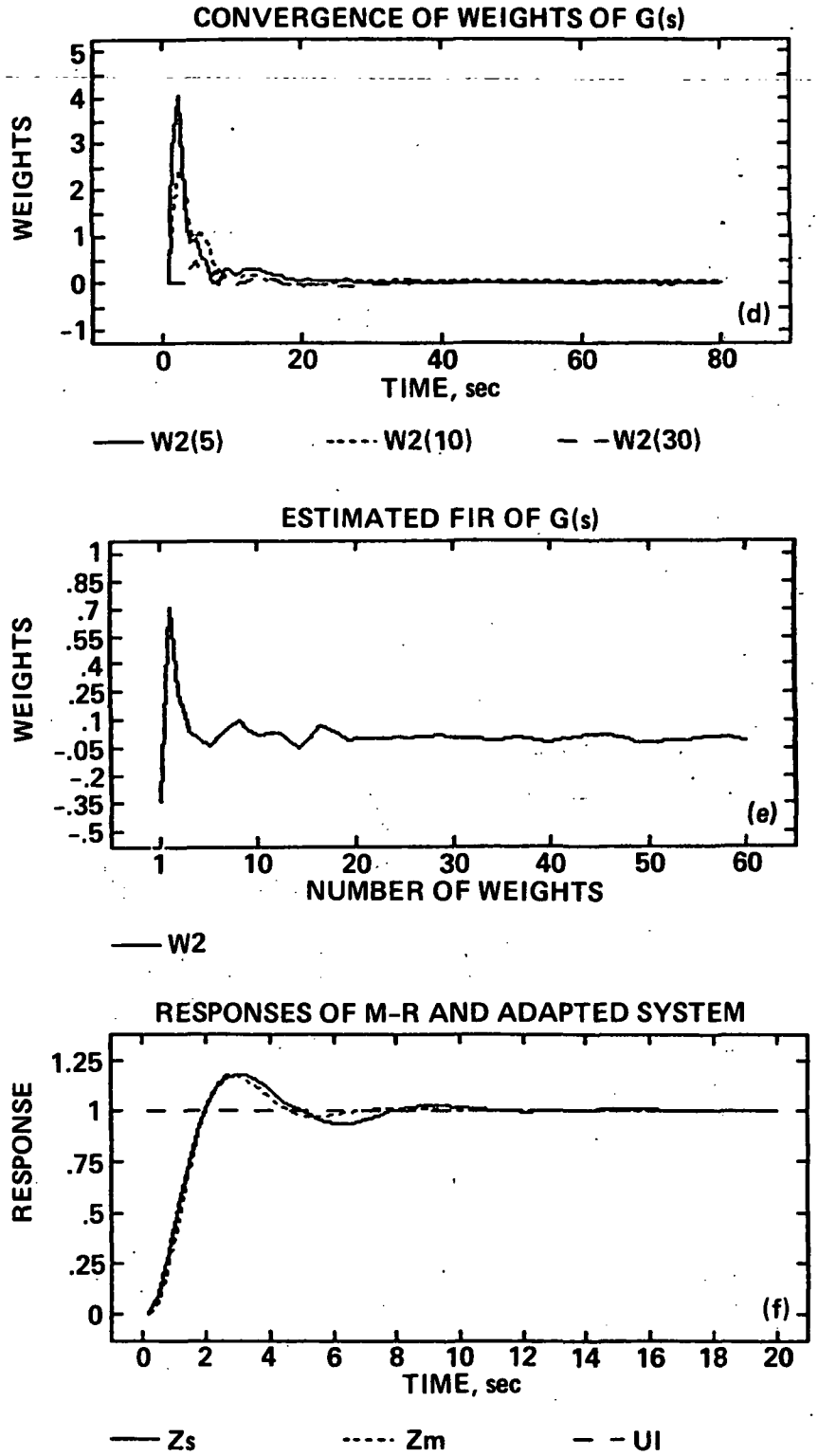

(d) Convergence history of the weights of G(s).

(e) Estimated FIR of G(s).

(f) Step responses of the reference model and the adapted system.

Figure 14.- Concluded.

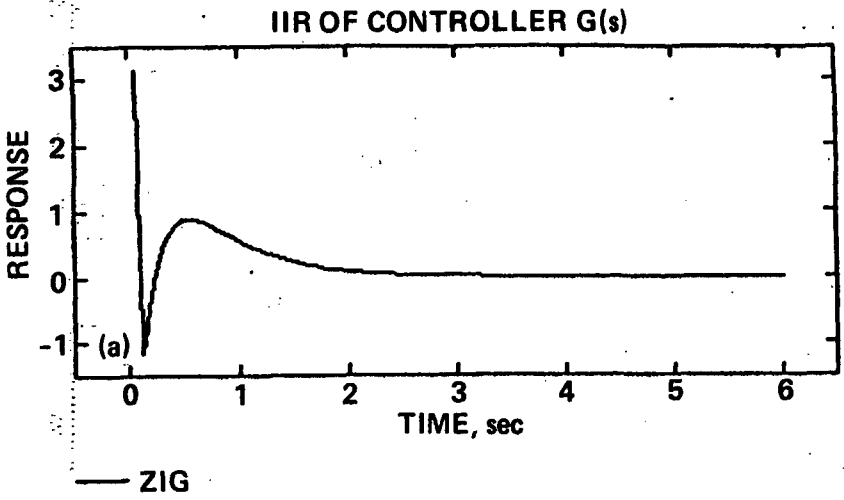

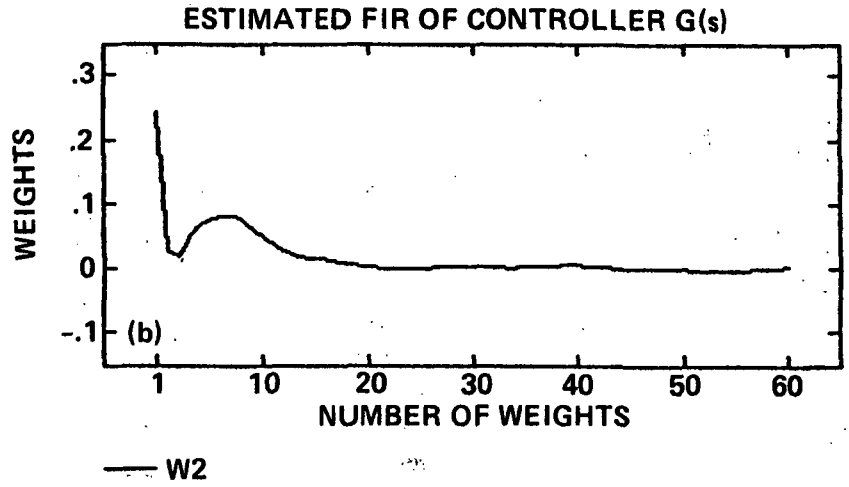

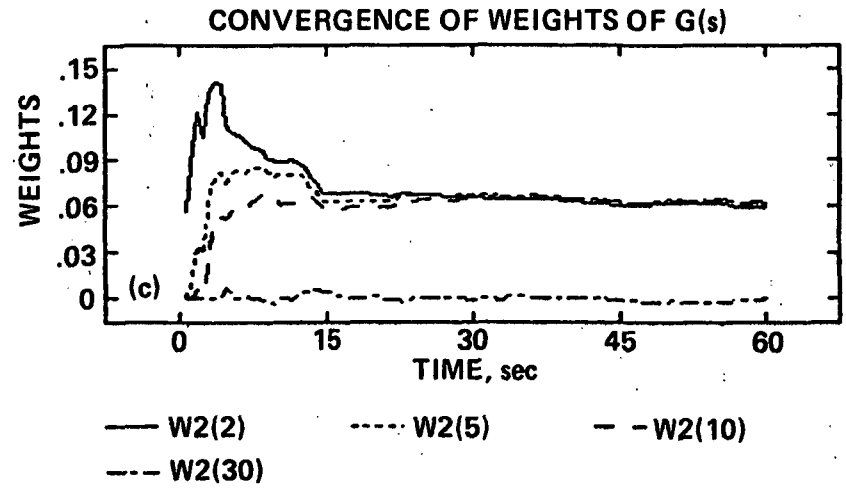

(a) Computed IIR of the controller G(s).

(b) Estimated FIR of the controller G(s).

(c) Convergence history of the weights of G(s).

Figure 15.- Configuration 3, $P(s) = 25/(s^2 + 1s + 25)$; band-limited excitation.

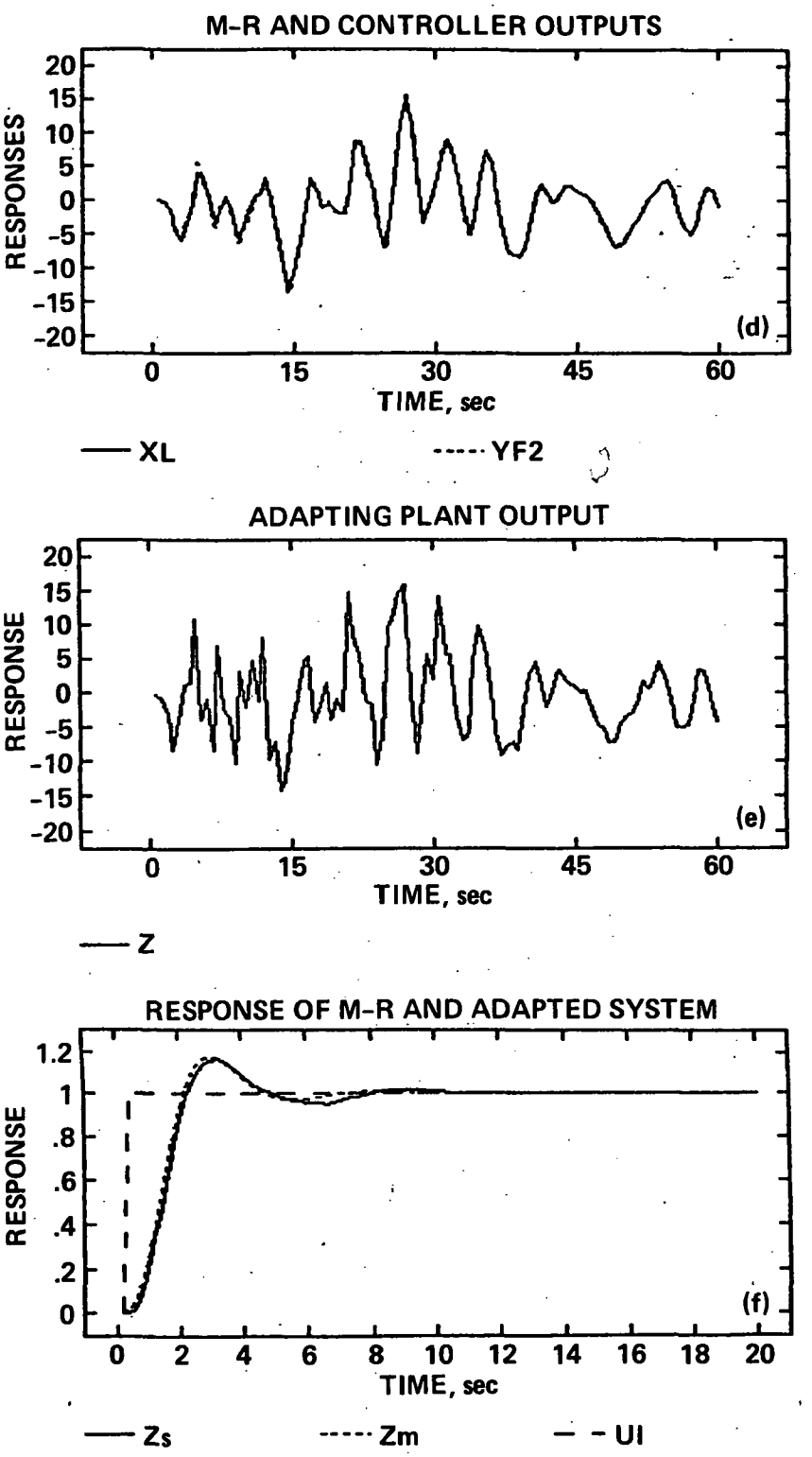

(d) Output histories of controller and reference model.

(e) Adapting plant output history.

(f) Step responses of the reference model and the adapted system.

Figure 15.- Concluded.

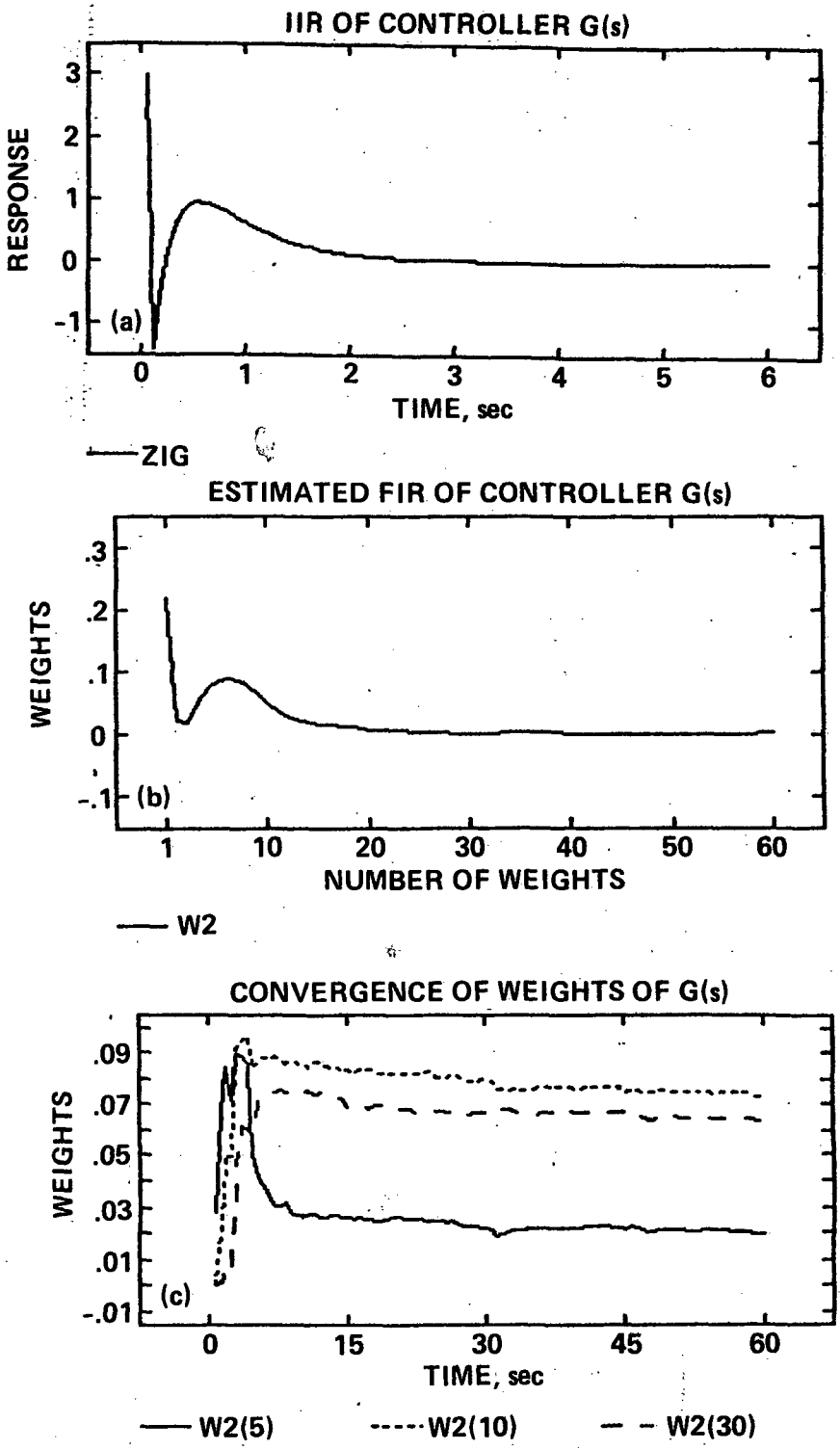

(a) Computed IIR of controller G(s).

(b) Estimated FIR of controller G(s).

(c) Convergence history of the weights of G(s).

Figure 16.- Configuration 3, $P(s) = 25/(s^2 + 0.1s + 25)$.

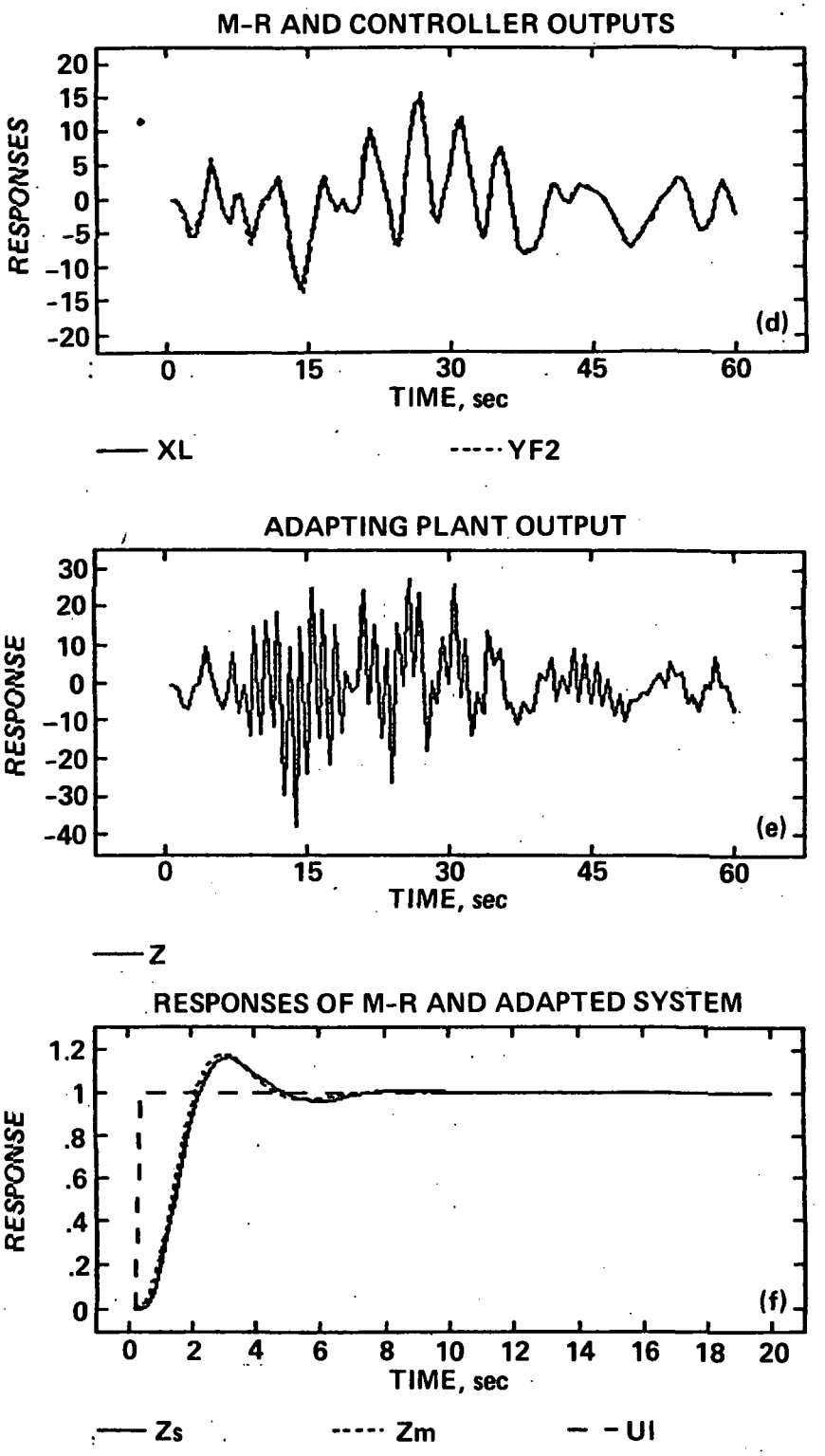

(d) Output histories of controller and reference model.

(e) Adapting plant output history.

(f) Step responses of the reference model and the adaptation system.

Figure 16.- Concluded.

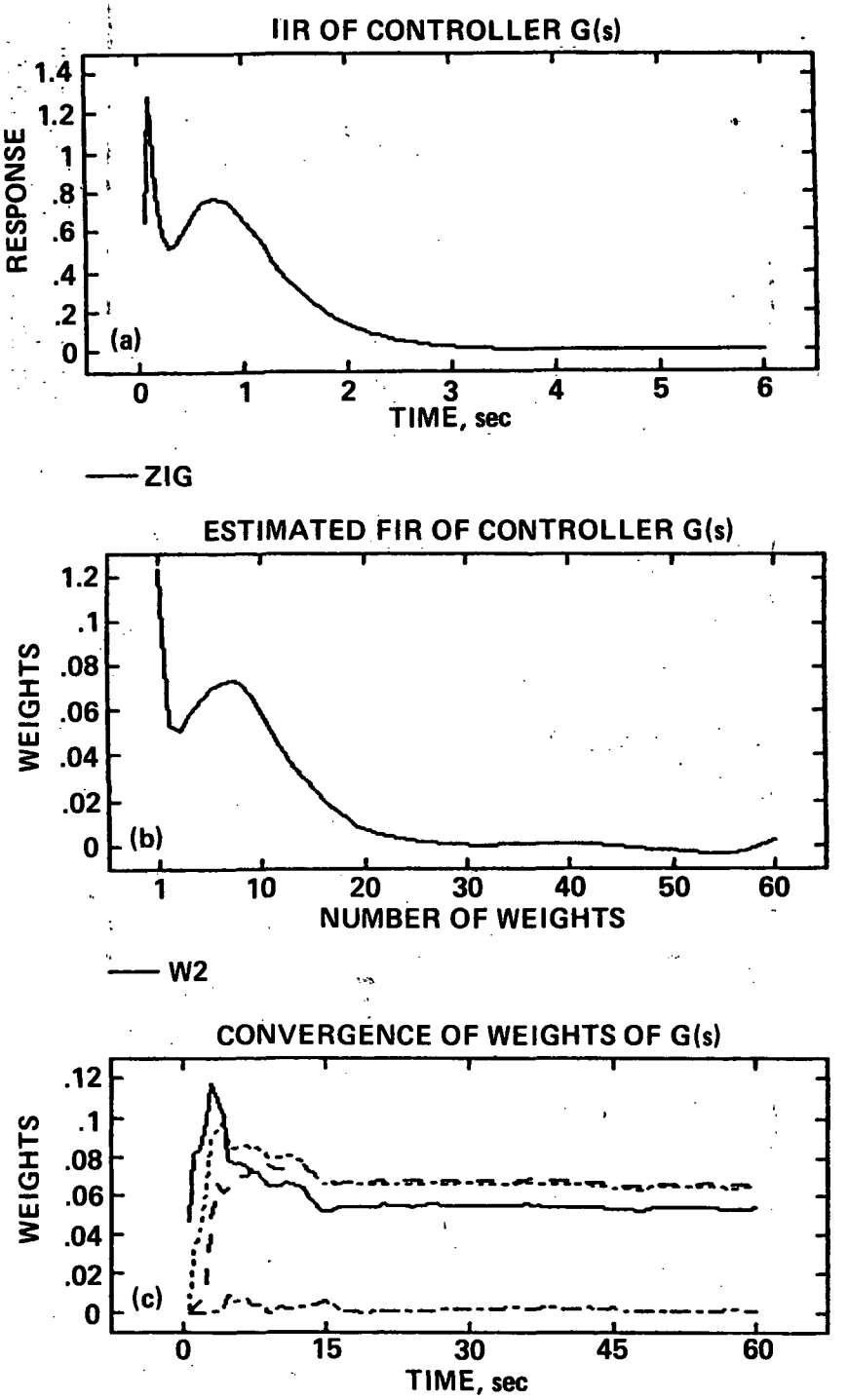

(a) Computed IIR of controller G(s).

(b) Estimated FIR of controller G(s).

(c) Convergence history of the weights of G(s).

Figure 17.- Configuration 3, $P(s) = 5(s + 5)/(s^2 + 2s + 25)$.

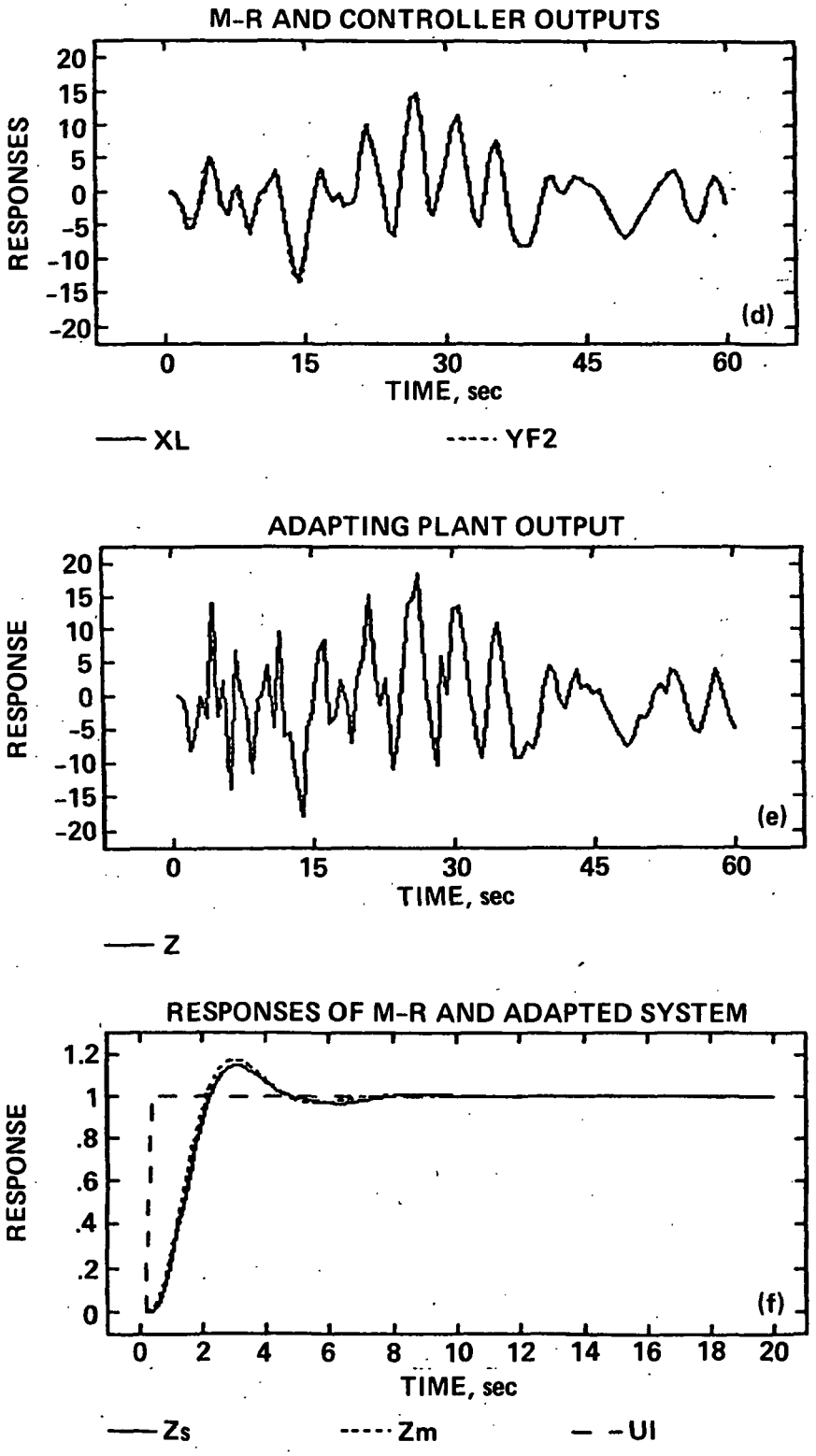

(d) Output histories of controller and reference model.

(e) Adapting plant output history.

(f) Step responses of the reference model and the adapted system.

Figure 17.- Concluded.

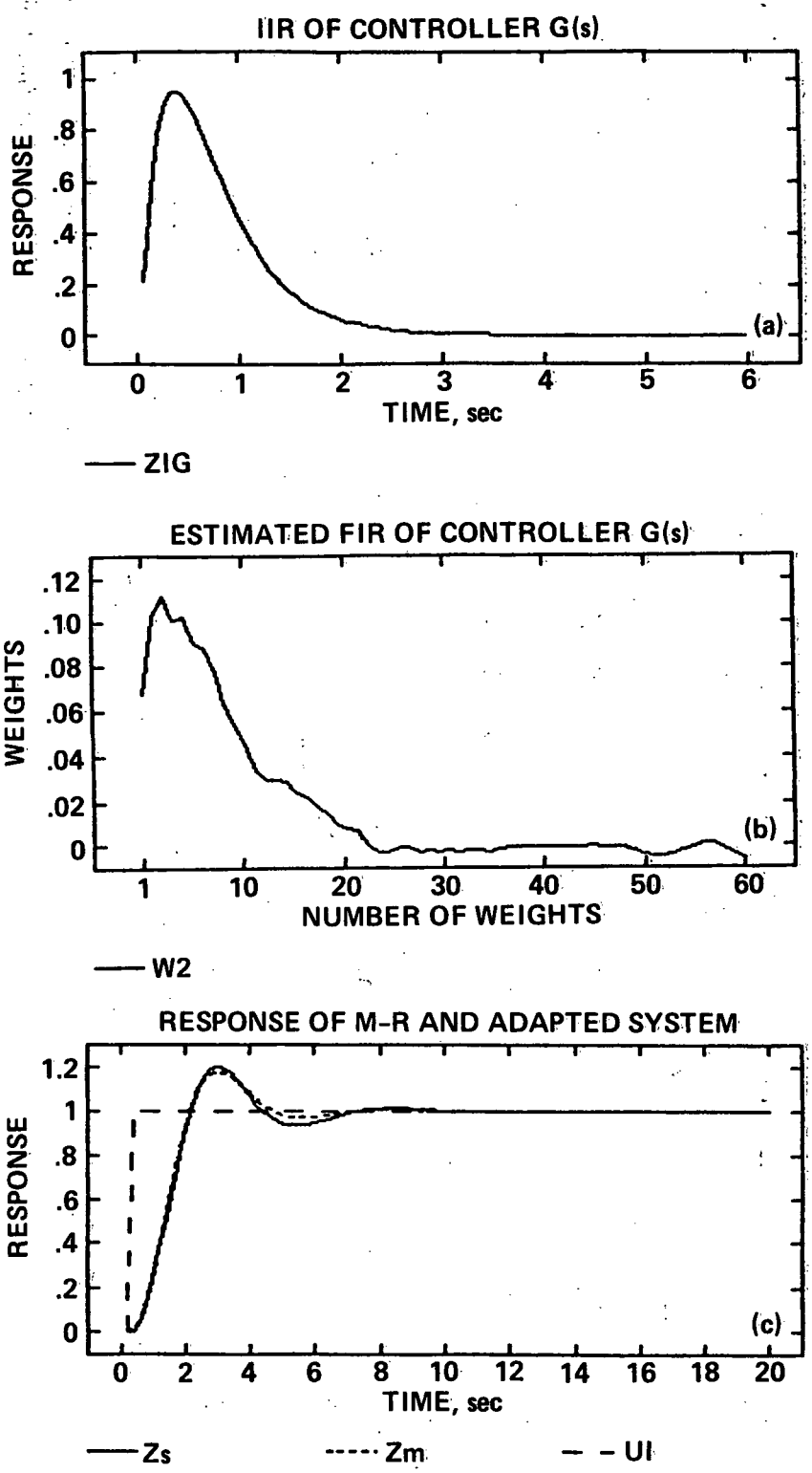

(a) Computed IIR of controller G(s).

(b) Estimated FIR of controller G(s).

(c) Step responses of the reference model and the adapted system.

Figure 18.- Configuration 3, $P(s) = 625/(s^2 + 5s + 625)$.

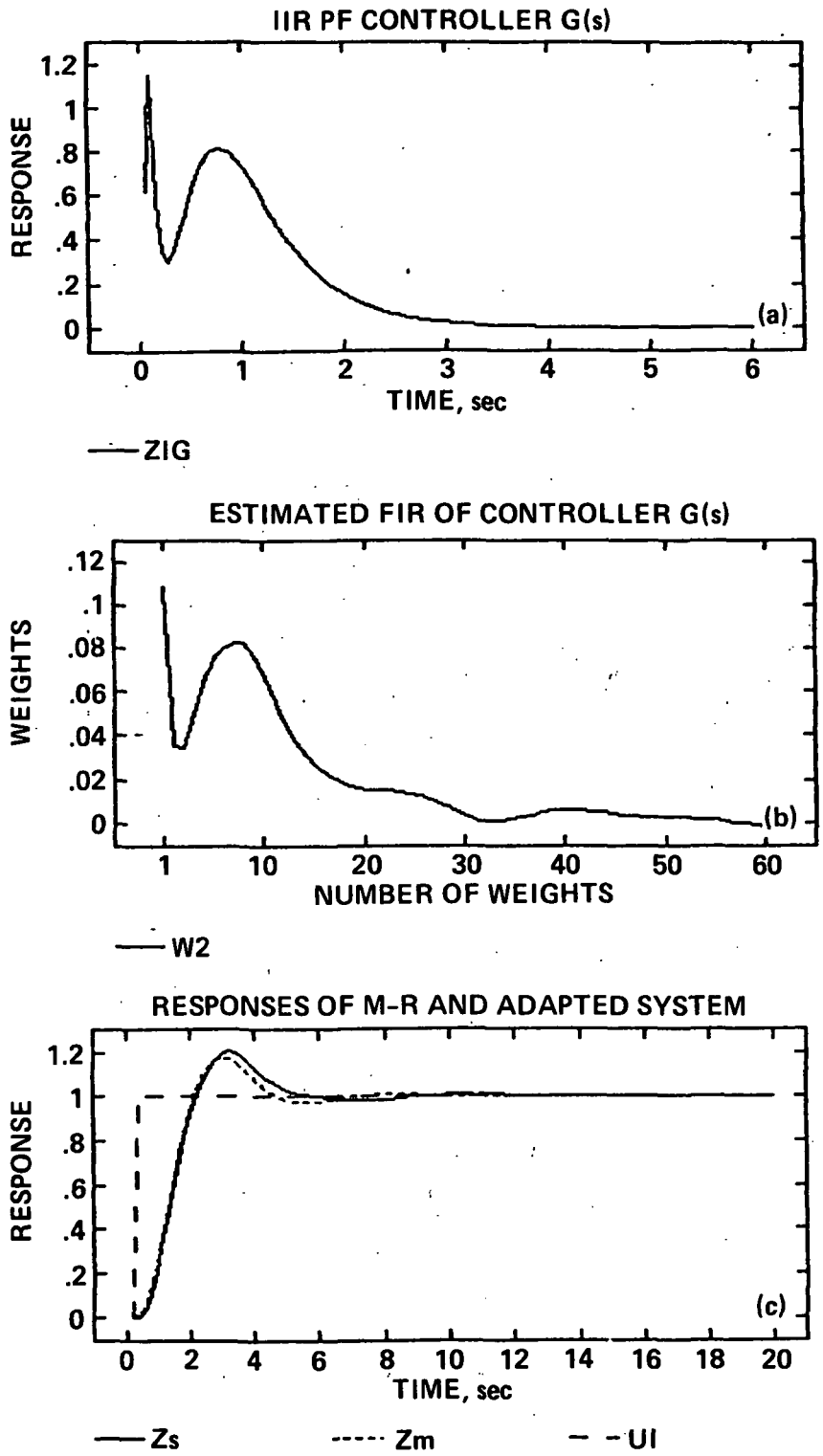

(a) Computed IIR of controller G(s).

(b) Estimated FIR of controller G(s).

(c) Step responses of the reference model and the adapted system.

Figure 19.- Configuration 3, $P(s) = 5(s + 5)/(s^2 + 0.01s + 25)$.

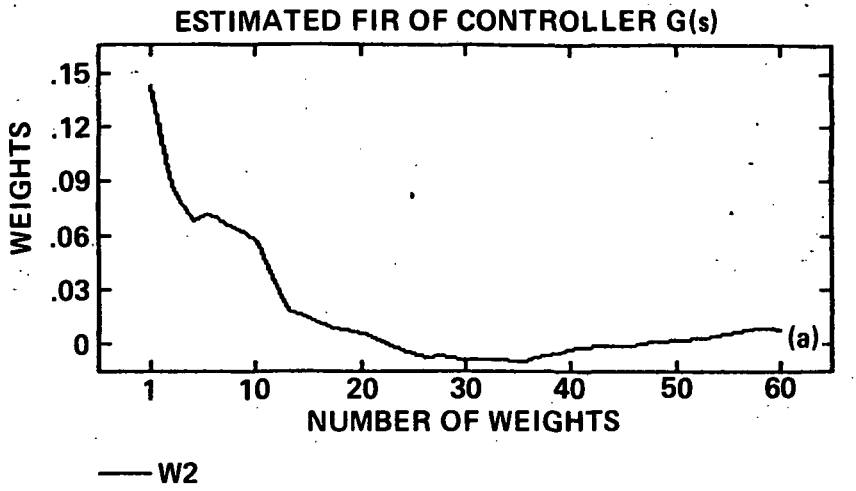

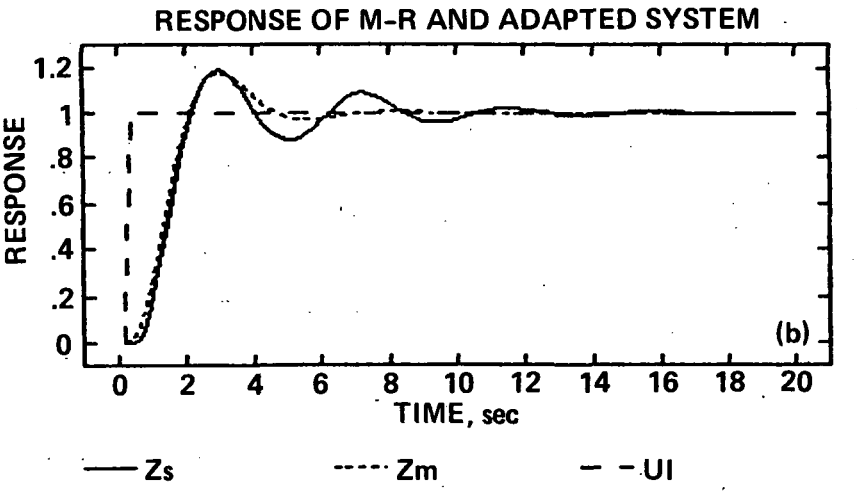

(a) Estimated FIR of controller G(s).

(b) Step responses of the reference model and the adapted system.

Figure 20.- Configuration 3, $P(s) = 25/(s^2 + 2s + 25)$; noise-to-signal ratio 0.05.

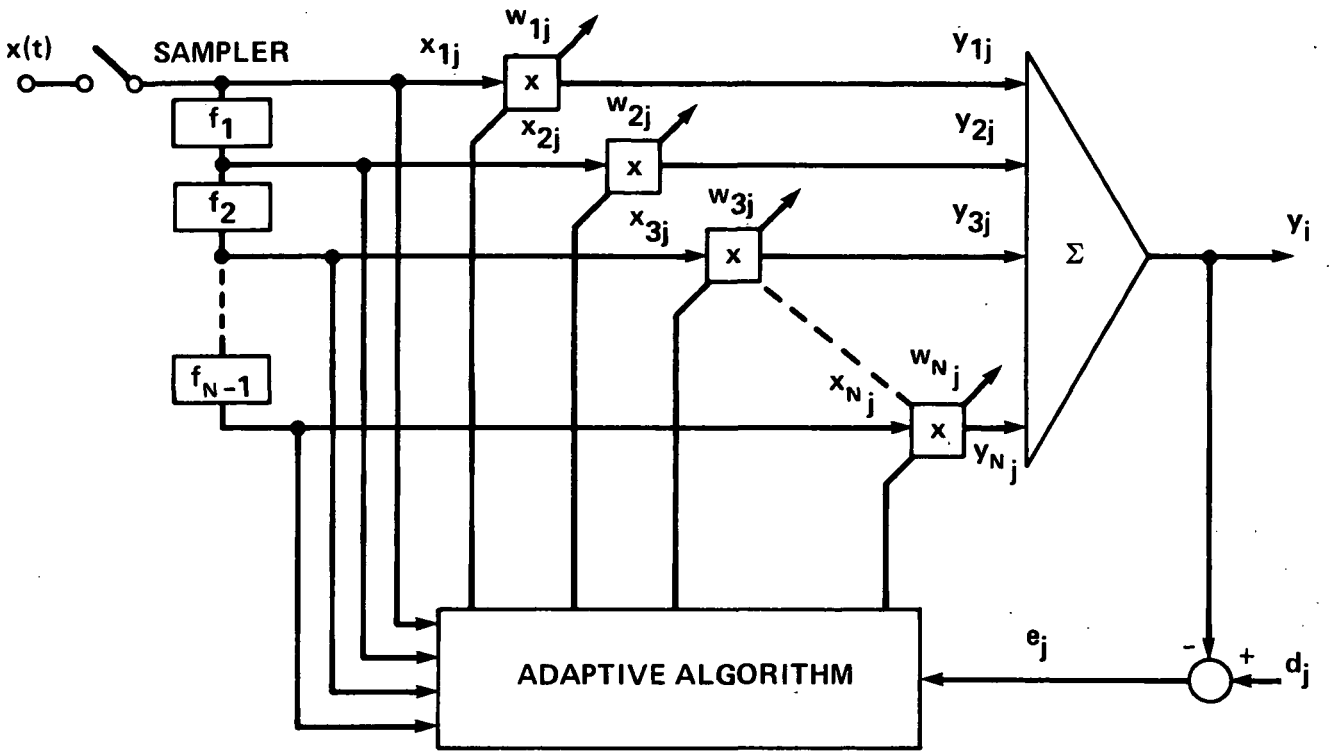

Figure A1.- Basic structure of a transversal self-adjusting (LMS) filter.

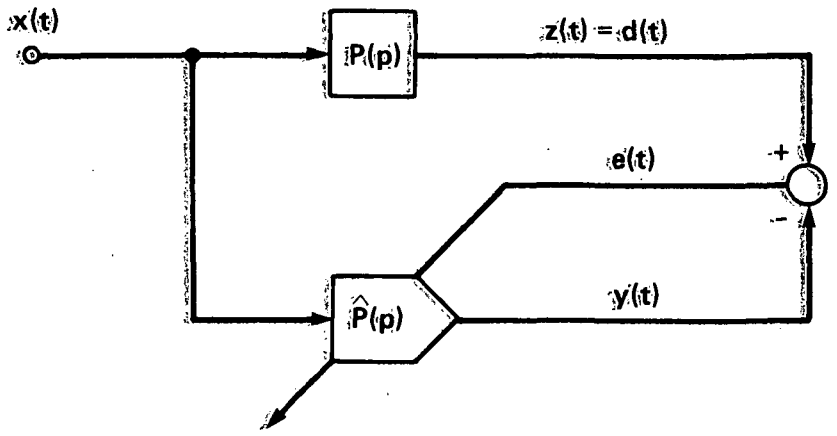

Figure A2.- Schematic representation of an LMS filter in the role of plant identification.

1. Report No.	2. Government Accession No.	3. Recipient's Catalog No.
NASA TM-86843		

4. Title and Subtitle	5. Report Date
DESIGN OF ADAPTIVE CONTROL SYSTEMS BY MEANS OF SELF-ADJUSTING TRANSVERSAL FILTERS	February 1986
	6. Performing Organization Code

7. Author(s)	8. Performing Organization Report No.
S. J. Merhav	A-85418
	10. Work Unit No.

9. Performing Organization Name and Address	11. Contract or Grant No.
Ames Research Center Moffett Field, CA 94035	
	13. Type of Report and Period Covered
12. Sponsoring Agency Name and Address	Technical Memorandum
National Aeronautics and Space Administration Washington, DC 20546	14. Sponsoring Agency Code 505-35-11

15. Supplementary Notes

Point of contact: Frank E. Neuman, Ames Research Center, MS 210-9, Moffett Field, CA 94035
(415)694-5431 or FTS 464-5431

16. Abstract

This paper addresses the design of closed-loop adaptive control systems based on nonparametric identification. Implementation is by self-adjusting Least Mean Square (LMS) transversal filters. The design concept is Model Reference Adaptive Control (MRAC). Major issues are to preserve the linearity of the error equation of each LMS filter, and to prevent estimation bias that is due to process or measurement noise, thus providing necessary conditions for the convergence and stability of the control system. The controlled element is assumed to be asymptotically stable and minimum phase. Because of the nonparametric Finite Impulse Response (FIR) estimates provided by the LMS filters, a priori information on the plant model is needed only in broad terms.

The "Indirect Method," involving explicit plant identification, and the "Direct Method," in which the controller is directly computed, are compared in the light of filter and system constraints. Following a survey of control system configurations and filter design considerations, system implementation is shown here in Single Input Single Output (SISO) format which is readily extendable to multivariable forms. In extensive computer simulation studies the controlled element is represented by a second-order system with widely varying damping, natural frequency, and relative degree. Excellent convergence and robustness are demonstrated by the step response of the adapted system which deviates from the reference model by only a few percent under wide parameter variations of the controlled element. Controller FIR estimates and convergence time-histories support the validity of the concept.

17. Key Words (Suggested by Author(s))	18. Distribution Statement
Control Estimation Adaptation Stability Noise	Unlimited Subject category - 66

19. Security Classif. (of this report)	20. Security Classif. (of this page)	21. No. of Pages	22. Price*
Unclassified	Unclassified	69	

*For sale by the National Technical Information Service, Springfield, Virginia 22161